DANISH METEOROLOGICAL INSTITUTE

SCIENTIFIC REPORT

02-16

Methodology for Risk Analysis based on Atmospheric Dispersion Modelling from Nuclear Risk Sites

Alexander Baklanov[1], Alexander Mahura[1,2]
Jens Havskov Sørensen[1], Olga Rigina[3], Ronny Bergman[4]

[1] Danish Meteorological Institute, Copenhagen, Denmark
[2] Institute of Northern Environmental Problems, Kola Science Centre, Apatity, Russia
[3] Technical University of Denmark, Lyngby, Denmark
[4] Swedish Defence Research Authority, Umeå, Sweden

'Arctic Risk' Project of the Nordic Arctic Research Programme (NARP)

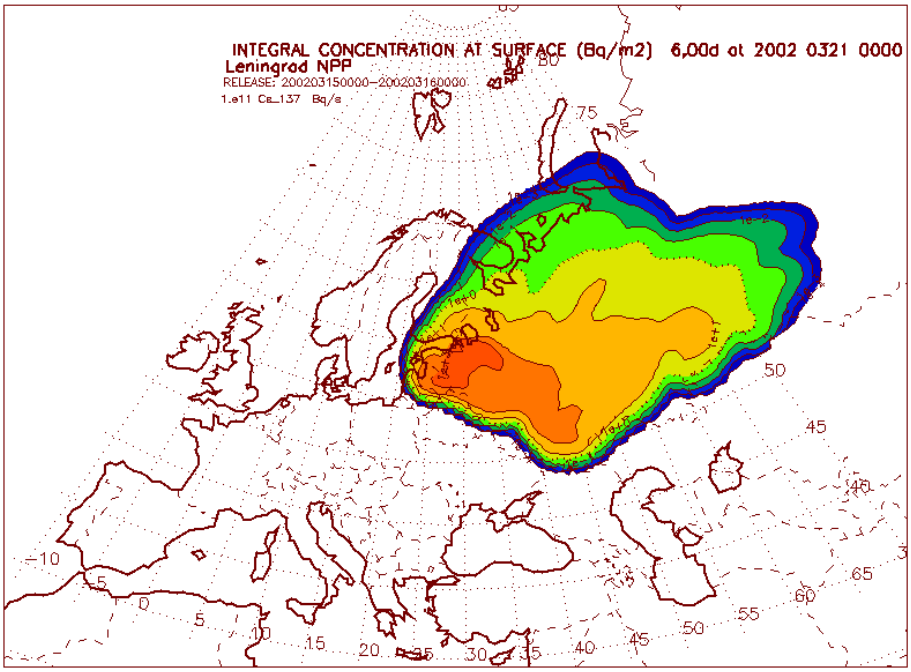

COPENHAGEN 2002

ISSN: 0905-3263 (printed)
ISSN: 1399-1949 (online)
ISBN: 87-7478-470-6

TABLE OF CONTENTS

SUMMARY

The risk for radioactive contamination and radiological consequences for an area is connected with the sources in this and adjacent areas. In some cases, they predominantly affect geophysical and social conditions at local and regional scales. In other cases, they appear to be far reaching, and of concern for larger territories. Thus, it is of particular interest to study issues such as: *Which sources appear to be the most dangerous now or in the future for people living close and far from these sources? Which geographical territories and countries are at highest risk from a hypothetical accidental release in a selected area?*

The main purpose of this multidisciplinary study is to develop a methodology for complex nuclear risk and vulnerability assessment and to test it on example estimation of a nuclear risk to the population in the Nordic countries in case of a severe accident at a nuclear risk site (NRS).

This report is focused on the methodology for evaluation of the atmospheric transport and deposition of radioactive pollutants from NRS's. The method for the evaluation is given from the probabilistic point of view. The main question to answer is: *What is the probability for radionuclide atmospheric transport and impact to different neighbouring regions and countries in case of an accident at NPPs?*

To answer this question we applied different research tools for probabilistic atmospheric studies: (i) Trajectory Modelling - 3-D isentropic trajectory model and 3-D DMI trajectory model – to calculate multiyear forward trajectories originated over the risk sites locations; (ii) Dispersion Modelling - DERMA & DMI-HIRLAM models – for long-term simulation and case studies of radionuclide transport for hypothetical accidental releases at NRS's; (iii) Cluster Analysis – to identify atmospheric transport pathways from NRS's; (iv) Probability Fields Analysis – to construct annual, monthly, and seasonal NRS possible impact indicators (based on both trajectory and dispersion modelling results) to identify the most impacted geographical regions; (v) Specific Case Studies – to estimate consequences for environment and population after hypothetical accident using DERMA and experimental dose models; (vi) Vulnerability Evaluation to Radioactive Deposition - concerning its persistence in the ecosystems with focus on transfer of certain radionuclides into food chains of key importance for the intake and exposure in the whole population and certain groups of the Nordic countries; (vii) Risk Evaluation and Mapping - to analyse socio-economical consequences for different geographical areas and various population groups taking into account social-geophysical factors and probabilities and using demographic databases based on the GIS-analysis.

In this report we consider aspects of the long-term dispersion and deposition modelling, statistical analysis of dispersion modelling results as well as briefly underline the methods for the dose calculation and assessment of regional vulnerability and residential radiation risk, based on GIS modelling and analysis.

The results of this study are applicable for the further GIS analysis to estimate risk and vulnerability as well as for the emergency response and preparedness measures in cases of accidental releases at NRS's.

I. INTRODUCTION

Nuclear risk in any geographical area is connected with nuclear sites in this or adjacent areas. The Chernobyl accident showed that the scale of impact can be very large, and remote nuclear risk sites should also be of considerable concern for the area. Thus, it is important to obtain the geographic distribution of the nuclear risk and to expound on issues such as:

- Which sources appear to be the most dangerous for people living close to and far from the sources?
- Which regions are at the highest risks from a hypothetical accidental release?

Many international research projects have realised models and methods describing separate parts of the problem, e.g. the probabilistic safety assessment (PSA), long-range transport and contamination modelling, radioecological sensitivity, dose simulation etc. However, methodologies for multidisciplinary work of nuclear risk assessments and mapping are poorly developed (for an overview cf. e.g. *Baklanov (2002)*). Thus, the next step should be a multidisciplinary approach towards problems connected to the regional nuclear risk and vulnerability.

The purpose of the ongoing Arctic Risk NARP study (*AR-NARP, 2001-2003*) is to develop a methodology for complex nuclear risk and vulnerability assessment and mapping, and to test it on estimation of a possible radiation risk to populations in the North European countries in case of a severe accident at a nuclear risk site (NRS).

In previous AR-NARP project reports (*Baklanov and Mahura, 2001; Mahura and Baklanov, 2002*) we described a general approach, methodology results of probabilistic analysis of atmospheric transport pattern and risk assessment based on trajectory modelling. In this report we will consider next step in the methodology of the regional risk and vulnerability assessment – the long-term dispersion modelling for the probabilistic analysis of risk and for the case studies.

For estimation of the potential nuclear risk and vulnerability levels, and for regional planning of radiological environmental monitoring networks and emergency preparedness systems, it is very important for each dangerous nuclear risk site to determine:

- geographical regions most likely to be impacted;
- probability and transport time to different geographical regions;
- probability and effects of the precipitation factor contribution by atmospheric layers;
- probability of the fast transport (in one day and less) when impact of the short-lived radionuclides is of the most concern;
- annual, seasonal and month variability of these parameters;
- worst meteorological scenarios for case studies;
- possible contamination and effects on the population in case of an accident;
- site-sensitive hazards of potential airborne radioactive release;
- vulnerability to a radioactive deposition concerning its persistence in the northern latitude ecosystems with a focus on the transfer of certain radionuclides into food-chains and considering risk for different geographical areas and especially native population;
- the analyses of the risk, socio-economical and geographical consequences for different geographical areas and population groups applying available demographic databases and GIS-technology.

In this report we consider aspects of the long-term dispersion and deposition modelling, statistical analysis of dispersion modelling results as well as briefly outline the methods for the dose calculation and assessment of regional vulnerability and residential radiation risk, based on GIS modelling and analysis (*Rigina, 2001; Rigina and Baklanov, 2002*).

II. METHODOLOGY FOR RISK ANALYSIS BASED ON ATMOSPHERIC DISPERSION MODELLING OF VARIOUS PATTERNS FROM NRS

2.1. *OVERVIEW OF PREVIOUSLY USED APPROACHES*

It is very important to develop a methodology for complex geographical multidisciplinary nuclear risk and vulnerability assessments suitable for the Arctic and Sub-Arctic regions. Risk-assessment strategy for analyses of source-effect relationships, used in different studies, includes the following main methods (*IIASA, 1996*):

1. INFERENCE FROM ACTUAL EVENTS: accident-release-consequences,
2. PHYSICAL MODEL based on known input and prevalent levels,
3. THEORETICAL MODEL: simulated response to assumed release scenarios.

The first method is basically used for most of the risk objects in the Northern regions using published results from some real events in this or other areas (weapon tests, the Chernobyl accident, the Thule accident with warheads, accidents with nuclear submarines like one in the Chazma bay, etc), discussed in (*IIASA, 1996*). For example, some long-term consequences have been estimated for regional-scale by empirical models and by correlations between fallout and doses for humans, obtained by Nordic researchers on a basis of the Chernobyl effects on Scandinavia (*Moberg, 1991, Bergman et al., 1993, Dahlgaard, 1994, Bergman & Ulvsand, 1994*).

The second method is used for many risk sites in the region. This method is also based on published results of numerous projects and assessments of possible risk levels for the Arctic and European regions or for some other countries from similar nuclear risk objects (see e.g., Chapters 3, 5 and 6 of *IIASA, 1996*).

Several case studies for hypothetical releases from the Kola and Loviisa NPPs, from nuclear submarines, or from radioactive waste deal with this issue by the third method: mathematical modelling (e.g., *Amosov et al., 1995; Rantalainen, 1995*).

An accident at a nuclear risk site might cause large releases of radioactive matters into the atmosphere. Then the resulting impact on people and the environment would largely depend on the prevailing weather conditions. Depending on the horizontal scale under study, a simulation of atmospheric transport, dispersion and deposition also demands different types of weather and release data. For the local scale (~10 km), wind structure, stability and information about the release, surface, building characteristics and precipitation are the most important parameters. For the meso-scale (~100 km), it is also important to include topography, different surface heating and cooling etc. For the regional scale (up to 4000 km), a good description of the synoptic evolution in time and space is also of importance. For this scale the only realistic way is to use numerical weather prediction or analyses data, whereas for simulations on local- and meso-scales it is often justified to use in-situ measurement data or modelled simplified weather conditions.

To study the possible consequences and nuclear risk from NRSs there could be *two approaches* – case studies & probabilistic risk analysis (*Rigina, 2001*). The *first approach* – case studies - is commonly used for estimation of possible dose for population and proceeds from the physical laws of radioactive matter transport from a nuclear reactor to man. This way is very useful for estimating possible consequences of hypothetical accidents for typical or worst-case scenarios and weather situations. However, such an approach was expensive for long-term (e.g. one or several years) simulations and probabilistic assessments and was inconvenient for an analysis of factors of different nature like, for example, geophysical processes of radionuclide transport and social-economical factors.

So, for probabilistic analysis, alongside with the first method, some authors suggested *simpler approaches*, e.g. based on a combination of different factors and probabilities of separate processes with appropriate weights.

The first map of risk in Europe due to severe accidents for all European NPPs (*Slaper et al., 1994*) mapped the probability of excess cancer mortality after such accidents. Since detailed safety analyses were not available for many of > 200 European NPPs, a generalisation was made to estimate accident probabilities and probabilistic releases by relating each reactor type to a specific probability and release category. Dispersion of the radioactive plume was evaluated by a simple model based on the only meteorological station. Acute health effects in the vicinity of the NPPs and counter measures to reduce radiation doses were excluded. This methodology was also used for the risk mapping from a nuclear submarine on the Kola Peninsula (*NACC, 1998*). The main shortcomings of this approach are a limitation of the dispersion model for short distances and non-applicability of the dose model to the Arctic peculiarity.

In IIASA studies (*Sinyak, 1995*) some empirical factors were used to describe the influences of geography resulting in normalised damage factors for the main cities of Europe. An alternative statistical description for estimating the risk associated with a large accidental release of hazardous materials at long range was developed by *Smith (1998)*.

Andreev et al. (*1998, 2000*) simulated dispersion and deposition with a Lagrangian particle model and calculated the frequency of exceedance of certain thresholds for the long-lived radionuclide ^{137}Cs, regarded as risk indicator. Sensitivity analysis demonstrated that the results strongly depended on the release frequencies. Additionally, GIS-based export/import matrices of risk were calculated for the European countries. Considerable shortcoming of this method is the use of a limited number of case studies /meteorological situations, which can not satisfactory represent the long-term statistics.

Jaffe et al. (1997), Mahura et al. (1999), Baklanov et al. (*1998, 2002*) used an isentropic trajectory model and cluster analysis technique for many-year period to assess possible impacts of a hypothetical nuclear accident in northern Europe. Long-term health consequences were estimated on the basis of the Chernobyl accident exposures in Scandinavia. Mapping of the regional nuclear risk and vulnerability was realised for Scandinavia by two different approaches based on integration of mathematical modelling and GIS-analysis (*Rigina and Baklanov, 2002*).

Saltbones et al. (2000) also realised the long-term trajectory analysis and case studies of long-range transport modelling for the Kola NPP, however they used two-dimensional trajectories and limited the study to the trajectory analysis with several case studies and did not realise the risk mapping.

For the purposes of risk mapping, following the above mentioned approaches (*Andreev et al., 1998, 2001; Rigina and Baklanov, 2002; Slaper et al., 1994; Kromp, 2002*), any risk indicator (*RI*) can be presented as a function of a scenario defined by a set of nuclear power plants, attributed source terms and release frequencies and can be described by the following term:

$$Aggr\{RI(x,y;r)\} = Aggr\left\{\sum_{i=1}^{N} Ps_i(r) * \sum_{j=1}^{M} Pm_j * DF\left[ST(RS_i,r) * SR_j(x,y;RS_i,r)\right]\right\},$$

where *RI* is risk indicator, *x, y* - geographical co-ordinates, *r* - reactor block, *RS* - release scenario, Ps_i - probability of release scenario *i*, Pm_j - probability of meteorological situation *j*, *M* - number of meteorological situations, ST_j - source term for release scenario RS_i and reactor *r*, *N* - number of release scenarios, *DF* - damage function, *SR* - source-receptor relationship.

The ongoing networking project ´Atmospheric Transport Pathways, Vulnerability and Possible Accidental Consequences from the Nuclear Risk Sites in the European Arctic (*Arctic Risk*)`,

involving 7 research groups from four Nordic countries and supported by the Nordic Arctic Research Programme (NARP), is aimed at developing and testing such a risk methodology for the Euro-Arctic region (*AR-NARP, 2001*). The methodology, developed in the bounds of the Arctic Risk project (*AR-NARP, 2001; Segerståhl et al., 2001; Baklanov et al., 2002,a; Rigina & Baklanov, 2002; Baklanov and Mahura, 2001*) is a logical continuation of several previous studies. Initially, the study of possible regional risk from the Kola Peninsula nuclear risk sites was started at the Kola Science Centre, Russian Academy of Sciences in 1991 in the bounds of the Russian State Programme 'Ecological Safety of Russia' of the Ministry of Environment, according to the Project 'RISK': 'Determination of risk zones and elaboration of scenarios of extreme radiologically dangerous situations in the Northern areas' and projects for the Kola NPP (*Baklanov et al., 1992, 1994; Amosov et al., 1995; Baklanov, 1995*). This study was continued in 1995-1997 and extended to the Kola-Barents region nuclear risk sites in a series of pilot studies/projects (e.g. the 'Kola Assessment Study') of the International Institute for Applied Systems Analysis (IIASA) and the Swedish Defence Research Establishment (FOA), under support of the Swedish Council for Planning and Coordination of Research (FRN). These studies were based on dispersion modelling, system analysis and ranging of possible risk from different nuclear risk sites in the Kola-Barents region (*Baklanov et al., 1996; IIASA, 1996; Bergman and Baklanov, 1998; Bergman et al., 1998; Baklanov and Bergman, 1999*). Other study was continued in 1996-1997 at the University of Alaska, Fairbanks for the Bilibino NPP using trajectory modelling and cluster analysis to evaluate atmospheric transport pathways to Alaska in the bounds of UAF-ADEC Joint Project (*Mahura et al., 1997a; Jaffe et al., 1997a; Mahura et al., 1999*). A similar study with a more complex approach for the statistical trajectory analysis and dispersion modelling for several specific cases was realised in 1997 for the Kola NPP in the bounds of the UAF-FOA-BECN Joint Project, sponsored by the Barents Environmental Centres Network (BECN) (*Mahura et al., 1997b; Jaffe et al., 1997b; Baklanov et al., 2001a*).

As the next step for multidisciplinary analysis of nuclear risk in the Barents Euro-Arctic Region, the 'Risk and Nuclear Waste in the Barents region' Programme (1998-2000) was initiated by the University of Umeå and FOA (*Baklanov and Bergman, 1998; ÖCB, 2000; Baklanov et al., 2001a; Mahura et al., 2001; Rigina and Baklanov, 1999; Baklanov et al., 2001b*). At the same period the INTAS Project (1998-2000) supplemented the *ÖCB* Project and involved additionally scientific groups from Russia (*Bergman, 1999; INTAS, 2000*). Additionally, a joint study of DMI and the Novosibirsk Computing Centre, Russian Academy of Sciences suggested an alternative method for estimation of nuclear risk and vulnerability, based on the sensitivity theory and inverse modelling (*Penenko and Baklanov, 2001*).

Therefore, the current 'Arctic Risk' NARP project (*Baklanov and Mahura, 2001; AR-NARP, 2001*) is a logical continuation and generalisation of the previous studies in this field. Each of the two basic approaches - the probabilistic assessments and the 'case study' - has some advantages and shortcomings, and neither of them is sufficient for the complex risk assessments. So, it was suggested (*Rigina and Baklanov, 2002; Baklanov and Mahura, 2001*) to use a combination of both methods, (§ 4.3, Figure 4.3.1: the probabilistic assessment and the case study), which gives a quite complex and non-expensive approach.

As it can be seen, many international research projects have elaborated models and methods solving separate parts of the problem, e.g. the probabilistic safety assessment (PSA), long-range transport and contamination modelling, radioecological sensitivity, dose simulation etc. However, methodologies for multidisciplinary work of nuclear risk assessments and mapping are poorly developed. So, the next step should be a multidisciplinary approach towards problems connected to the regional nuclear risk and vulnerability (*Baklanov, 2002*). *As recommendations for further studies* in complex nuclear risk assessments and mapping in the Arctic and Sub-Arctic, we can

suggest the following optimal strategy for multidisciplinary methodology, that integrates different specific approaches of several authors:

a) using a combination of the probabilistic analysis and case studies (*Rigina, 2001; Baklanov et al., 2002)*;
b) probabilistic approach for airborne risk studies (*Baklanov and Mahura, 2001*);
c) radio-ecological sensitivity and specific pathways for the Arctic (*Bergman and Ågren, 1999; Wright et al., 1997, 2002; Selnas & Strand, 2002; Travnikova et al., 2002; Howard et al., 2002*);
d) PSA and probability of different severity accidents (*Fullwood, 1999; Webler et al., 1991; Slaper et al., 1994; IAEA, 1992, 1995, 1996)*;
e) possible economical loss and consequences (*Segerståhl, 1991; Slaper et al., 1994; Andreev et al., 2000; OTA, 1995)*;
f) integration in GIS for risk and vulnerability mapping (*Rigina, 2001; Rigina and Baklanov, 2002; Baklanov et al., 2002)*.

2.2. *APPROACH FOR RISK ANALYSIS PROPOSED IN THIS STUDY*

The suggested scheme for complex multidisciplinary risk assessment, which includes a combination of dispersion modelling and statistical analysis in comparison with the trajectory modelling and statistical analysis of trajectories, is shown in Figure 2.2.1. For assessment of risk and vulnerability we consider different *indicators* including the *social-geophysical factors*, which depend on the location and population of the area of interest:

- proximity to the radiation risk sites;
- population density in the area of interest;
- presence of critical groups of population;
- ecological vulnerability of the area;
- risk perception, preparedness of safety measures, systems for emergency response;

and *probabilities*:

- probability of an accident of a given severity at the NRS;
- probability of air transport pathways towards the area of interest from the NRS (from probabilistic trajectory modelling);
- probability of precipitation and deposition over the area of interest during the transport of the plume (from probabilistic dispersion modelling).

For estimation of vulnerability and risk for different regions, a risk function is defined as a complex index of probability of risk for different factors (*Rigina & Baklanov, 2002*). There could be two methods to define such a function. The first method is commonly used for the estimation of the possible dose for a population, and it proceeds from the physical laws describing the transport of radioactive matter from a nuclear reactor to man. This method is more expensive in computation due to the necessity of dispersion modelling. Besides, it is inconvenient for analysis of factors of different nature, for example, geophysical processes of radionuclide transport and social-economical factors. Thus, along with the first method, we suggest a simpler and more universal method, which is based on a combination of different factors/indicators and probabilities of individual processes. In this case, we express the total risk function for an administrative unit as the sum of complex risks from each of the major radiation risk sites in the region. For each site, the risk is defined by two different formulations. The first formulation supposes a multiplication of different factors and probabilities, and the second formulation involves a multiplication of risk probabilities and a weighted sum of other factors.

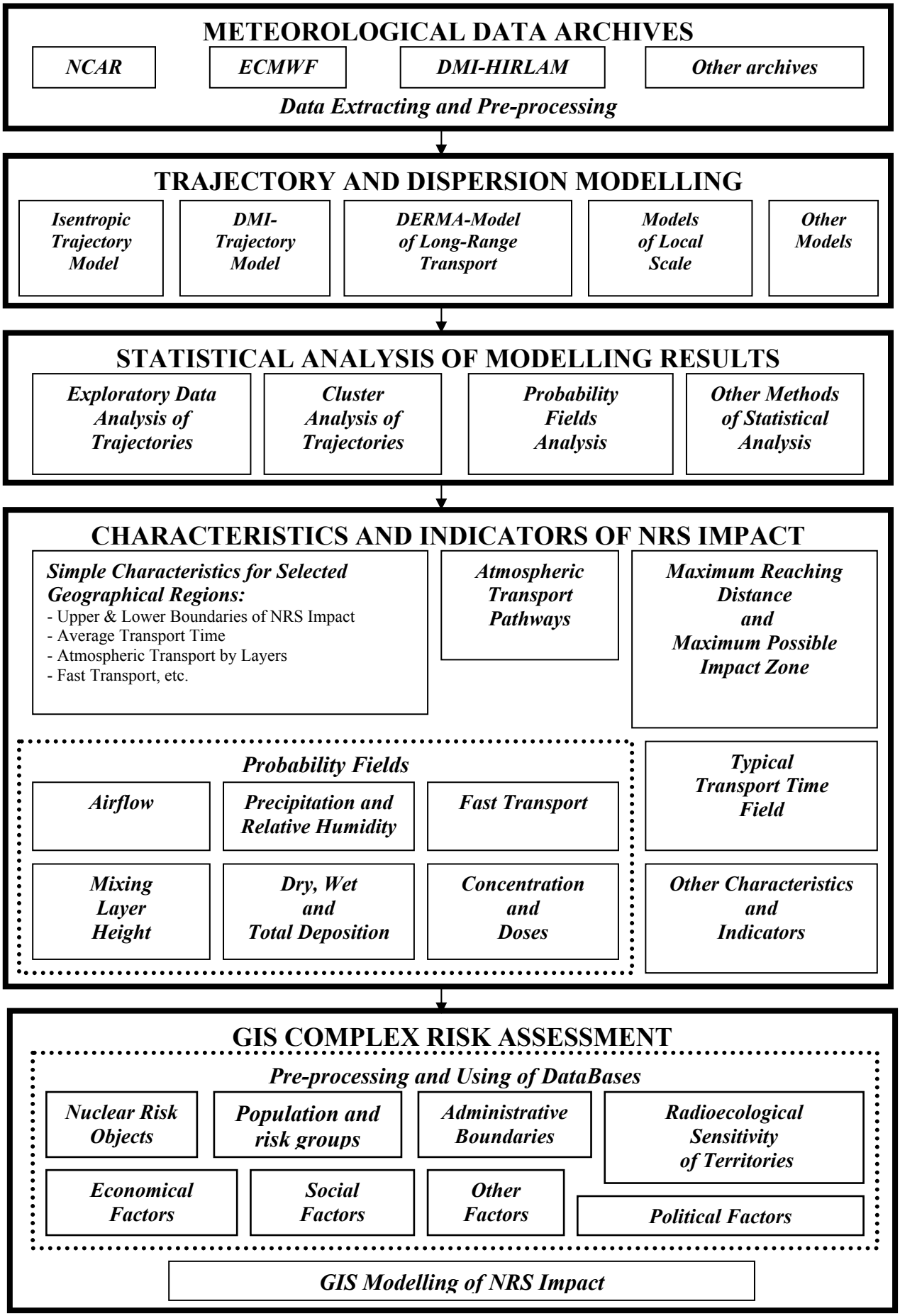

Figure 2.2.1. Scheme of the probabilistic risk analysis based on dispersion and trajectory modelling approaches.

APPROACHES

As shown in Fig. 2.2.1, there is a variety of research tools in the methodology scheme of probabilistic complex risk and vulnerability assessments. In this report, we describe the suggested multidisciplinary approach and illustrate a few of the tools involved. Necessary to note that other approaches also include clustering of trajectories, specific case studies, and evaluation of vulnerability to radioactive deposition. In this study, we use the following models and approaches (*AR-NARP, 2001-2003; Baklanov & Mahura, 2001; Baklanov et al., 1998, 2002; Mahura et al., 1999, 2001; Rigina & Baklanov, 2002*):

- Trajectory modelling - 3-D isentropic trajectory model (*Merrill et al., 1985*) and 3-D DMI trajectory model (*Sørensen et al., 1994*) - calculates multiyear forward trajectories originated over NRSs;
- Cluster analysis technique (*Jaffe et al., 1997a; Mahura et al., 1999; Baklanov et al., 2002*) - identifies atmospheric transport pathways from NRSs;
- Probability fields analysis (*Jaffe et al., 1997b; Baklanov et al., 1998; Baklanov & Mahura, 2001; Mahura 2001*) - constructs monthly and seasonally airflow, fast transport and precipitation factor probability fields to identify the most impacted geographical regions;
- Long-range transport - DERMA (*Sørensen, 1998; Baklanov and Sørensen, 2001*) and DMI-HIRLAM (*Sass et al., 2000*) models - simulate radionuclide transport for hypothetical accidental releases at NRSs;
- Specific case studies – estimate consequences for the environment and population after hypothetical accidents using experimental models based on the Chernobyl effects for the Nordic countries (*Moberg, 1991; Dahlgaard, 1994; Nielsen, 1998; Bergman & Ågren, 1999; Baklanov et al., 2002*);
- Evaluation of vulnerability to radioactive deposition - concerning its persistence in the ecosystems with a focus on transfer of certain radionuclides into food chains of key importance for the intake and exposure in the whole population and certain groups in the Nordic countries (*Bergman and Ågren, 2000*);
- Complex risk evaluation and mapping - using demographic databases in combination with the GIS-analysis (*Rigina & Baklanov, 1999, 2002; Rigina, 2001*) - estimate socio-economical consequences for different geographical areas and various population groups taking into account: 1) social-geophysical factors (proximity to NRSs, population density; critical groups of population; ecological vulnerability of area; risk perception, preparedness of safety measures and quick response systems; counteracting economical and technical consequences of accident) and 2) probabilities (accident of certain severity; atmospheric transport from NRSs; removal over area during atmospheric transport).

If we assume either a unit puff release or continuous release every 12 hours at an NRS, and run a model of atmospheric transport, dispersion, and removal of the radioactive material, we can produce a field for the wet deposition accumulated during a multiyear period. From one side, we can estimate what would be accumulated deposition if a continuous release took place. From another side, we can identify the geographical areas, presumably of the cellular nature. These areas are the territories where the greatest removal of radionuclides is possible during transport from the site. It should be noted that such fields are also (as in the previous approach) valid with respect to the particular NRS of interest.

Additionally, useful information can be obtained if we have the averaged climatological airflow patterns for the regional or local scale. We can evaluate seasonal and monthly average wet deposition factor fields applying averages for wind characteristics, precipitation, temperature, relative humidity, etc. For this case, the averaged 3-D meteorological fields are simulated, and then they are used in the transport model to calculate such characteristics as the air concentration, surface deposition, and doses. Specific cases for both unit and hypothetical, such as maximum possible accident (MPA), releases can be considered. Additional cases of unfavourable meteorological conditions can be evaluated too (*INTAS, 2000; ÖCB, 2000*). Produced characteristic monthly or seasonal fields of the air concentration, deposition, and various doses could be used in the decision-making process at the first stages of an NRS accident.

As we discussed above, the dispersion and deposition models can be successfully used for separate case studies for typical or worst-case scenarios, as well as for probabilistic risk mapping (as a more expensive but preciser alternative of the trajectory analysis method). Applicability and examples of different models for accidental release dispersion and deposition simulation for the local and regional scales were discussed in our previous publications (*Baklanov et al., 1994; Thaning and Baklanov, 1997; Baklanov, 2000; Baklanov et al., 2001; Baklanov and Sørensen, 2001*).

At DMI we have already developed a useful methodology within the 'Arctic Risk' NARP project and we have tested some methodological aspects for a hypothetical accidental radioactive release from the nuclear submarine Kursk during its lifting and transportation to the harbour on the Kola Peninsula. The Kursk Nuclear Submarine Pilot Study results were presented in *Mahura et al. (2002), Baklanov et al. (2002)* and available on a CD-room data base (*AR-NARP, 2001*) on a request to DMI.

The methodology of the probabilistic trajectory analysis and calculation of different risk indicators based on the trajectory modelling (see the scheme in Figure 2.2.1) was described in the previous project report (*Baklanov and Mahura, 2001*). Therefore, the methodology of dispersion modelling for the probabilistic analysis (Figure 2.2.1) with applications to different nuclear risk sites in the European North is the main topic of this report.

2.3. *NUCLEAR RISK SITES OF INTEREST FOR THE STUDY*

One of the main items of this study is to prepare the methodology for the further risk assessment of the selected nuclear risk sites in the Euro-Arctic region. These sites include nuclear power plants (NPPs) in Russia, Lithuania, Germany, United Kingdom, Finland, Ukraine, and Sweden (see Table 2.3.1, Figure 2.3.2).

Nuclear Risk Sites

All the selected sites are located within the area of interest of the "Arctic Risk" Project. Moreover, the Kola NPP (KNP, Murmansk Region, Russia) has the old type of reactors (VVER-230); Leningrad (LNP, Leningrad Region, Russia), Chernobyl (CNP, Ukraine), and Ignalina (INP, Lithuania) NPPs have the most dangerous RBMK-type reactor; Novaya Zemlya (NZS, Novaya Zemlya Archipelago, Russia) was considered as the former nuclear weapon test site and potential site for nuclear waste deposit; and the Roslyakovo shipyard (KNS, Murmansk Region, Russia) was considered as a risk site with nuclear power ships in operation or waiting to be decommissioned.

Table 2.3.1. Nuclear risk sites selected for the "Arctic Risk" Project.

#	Site	Lat,°N	Lon,°E	Site Names	Country
1	***KNP***	67.75	32.75	Kola NPP	Russia
2	***LNP***	59.90	29.00	Leningrad NPP	Russia
3	***NZS***	72.50	54.50	Novaya Zemlya Test Site	Russia
4	***INP***	55.50	26.00	Ignalina NPP	Lithuania
5	***BBP***	54.50	-3.50°W	Block of the British NPPs	United Kingdom
6	***BGP***	53.50	9.00	Block of the German NPPs	Germany
7	***LRS***	60.50	26.50	Loviisa NPP	Finland
8	***TRS***	61.50	21.50	Olkiluoto (TVO) NPP	Finland
9	***ONP***	57.25	16.50	Oskarshamn NPP	Sweden
10	***RNP***	57.75	12.00	Ringhals NPP	Sweden
11	***BNP***	55.75	13.00	Barsebaeck NPP	Sweden
12	***FNP***	60.40	18.25	Forshmark NPP	Sweden
13	***KRS***	51.70	35.70	Kursk NPP	Russia
14	***SNP***	54.80	32.00	Smolensk NPP	Russia
15	***CNP***	51.30	30.25	Chernobyl NPP	Ukraine
16	***KNS***	69.20	33.40	Roslyakovo Shipyard	Russia

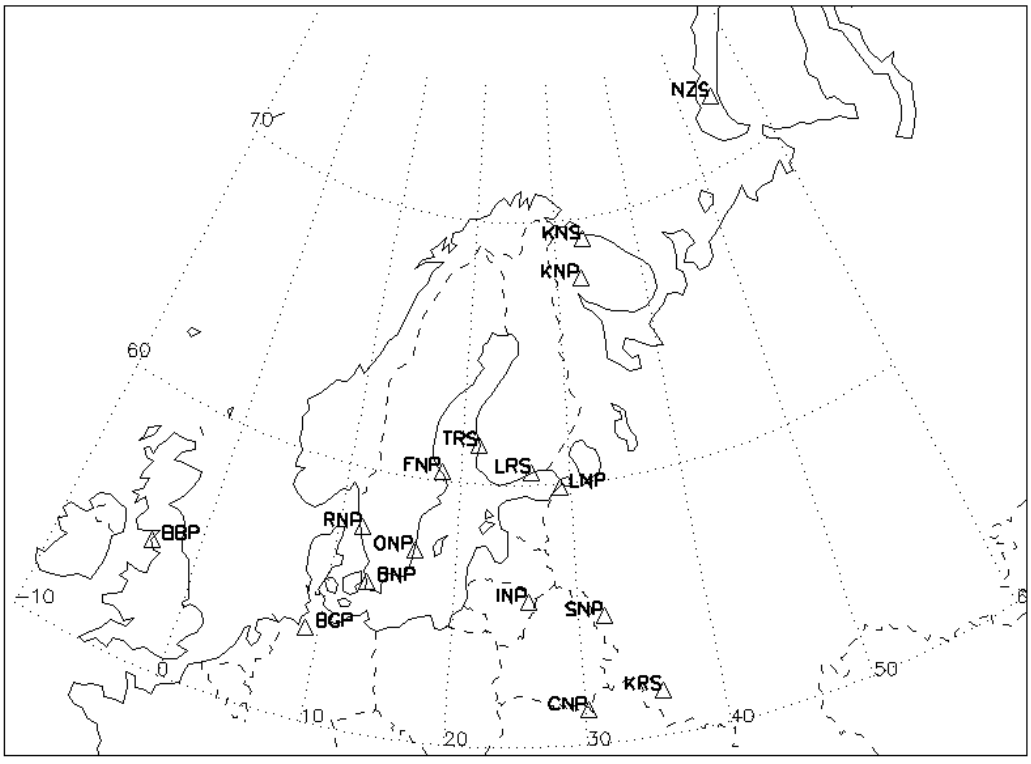

Figure 2.3.2. Selected nuclear risk sites for dispersion modelling.

The Block of the British NPPs (BBP) is represented by a group of the risk sites: Chapelcross (Annan, Dumfriesshire), Calder Hall (Seascale, Cumbria), Heysham (Heysham, Lancashire), and Hunterston (Ayrshire, Strathclyde) NPPs and the Sellafield reprocessing plant. The Block of the German NPPs (BGP) is represented by a group of NPPs: Stade (Stade, Niedersachsen), Kruemmel (Geesthacht, Schleswig-Holstein), Brunsbuettel (Brunsbuettel, Schleswig-Holstein), Brokdorf (Brokdorf, Schleswig-Holstein), and Unterweser (Rodenkirchen, Niedersachsen). Although these NPPs use different reactor types and, hence, could have different risks of accidental releases, the grouping is relevant for airborne transport studies because all NPPs are located geographically close to each other and, hence, atmospheric transport patterns will be relatively similar.

III. METHODOLOGY FOR LONG-TERM DISPERSION MODELLING

The main focus of this report is to describe the methodology developed for the probabilistic atmospheric studies based on the long-term dispersion modelling for the risk assessment of nuclear risk sites. Depending on the scale considered - local, regional or global - different atmospheric dispersion models can be used. The DERMA model is used for meso- and long-range transport simulations.

3.1. *DESCRIPTION OF THE DERMA MODEL*

The **D**anish **E**mergency **R**esponse **M**odel for **A**tmosphere (**DERMA**) is a numerical three-dimensional atmospheric dispersion model of Lagrangian type. This model describes atmospheric transport, diffusion, deposition, and radioactive decay within a range from about 20 kilometres to the global scale. DERMA is developed at the **D**anish **M**eteorological **I**nstitute (**DMI**) for nuclear emergency preparedness purposes and integrated with the ARGOS system (see Figure 3.1.1). This model uses **N**umerical **W**eather **P**rediction (**NWP**) model data from different operational versions of the **HI**gh **R**esolution **L**imited **A**rea **M**odel (**HIRLAM**) running at DMI or from the global model of the European Centre for Medium-Range Weather Forecast (ECMWF). The DERMA model structure and its dispersion modelling block were described by *Sørensen (1998)* and *Sørensen et al. (1998)*, and the deposition modelling block – by *Baklanov & Sørensen (2001*).

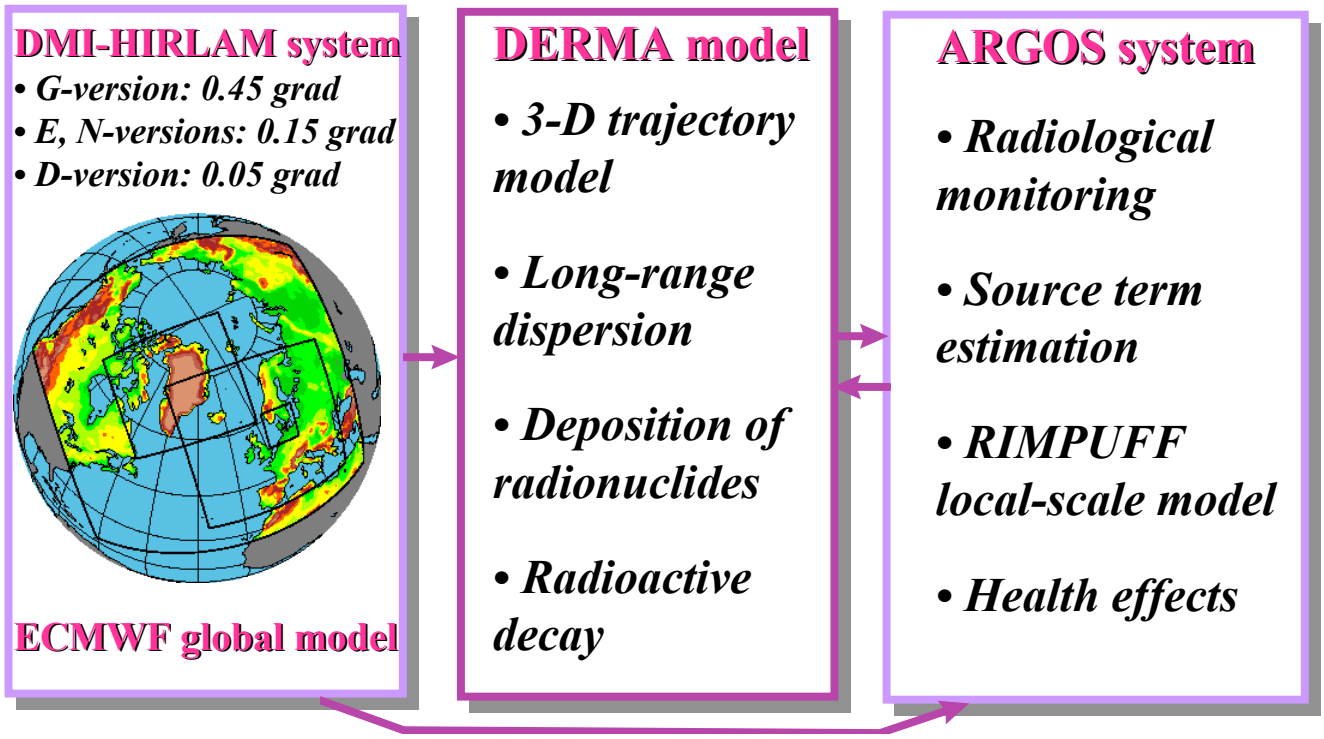

Figure 3.1.1. Structure of the Danish nuclear emergency preparedness long-range modelling system.

Earlier comparisons of simulations by the DERMA model vs. the ETEX experiment involving passive tracers showed very good results. Institutions (in total 28) from the European countries, USA, Canada, and Japan contributed to the real-time model evaluation. Based on analyses from this

experiment, the DERMA model was emphasised as being very successful (*Graziani et al., 1998*). In order to verify the deposition parameterisations and study effects of deposition, DERMA simulations for several cases – (the INEX and RTMOD exercises, and Algeciras accidental ^{137}Cs release in Spain) – were conducted taking into account different approaches for the deposition processes. In particular, the comparison of simulation results for the Algeciras accidental release with measurement data from the European monitoring network were analysed by *Baklanov (1999)* and *Baklanov & Sørensen (2001)*.

The basic equation for concentration of radioactive species in the atmosphere, c, taking into account the removal processes in the atmosphere and the interaction of the radionuclides with the Earth's surface, can be expressed:

$$\frac{\partial c}{\partial t} = -div(\mathbf{u}\, c) + Turb - Ddep - Wdep - \lambda c + \lambda' c' + Res + Q, \qquad (1)$$

where:

$div(\mathbf{u}\, c)$ - advection transport by vector velocity $\mathbf{u}$,
Turb - turbulent diffusion of passive tracers in the atmosphere,
Ddep - dry deposition on the surface,
Wdep - wet deposition processes,
λc - radioactive decay to daughter nuclides,
$\lambda' c'$ - decay from parent nuclides,
λ - decay constant for the corresponding nuclide,
Res - resuspension processes,
Q - release source.

For nuclear emergency response and post-accidental analysis, several versions of the DERMA model including different approaches and complexity of parameterisations of the deposition processes can be used. Let us describe the version of the DERMA model which was selected for the long-term simulation of contamination.

The temporal resolution of the currently available operational NWP model data is one or few hours. The DERMA model interpolates these data linearly in time to the advection time steps. The advection time step of DERMA is equal to e.g. 15 minutes (which is a typical turn-over time of the large vertical eddies within the boundary layer of the atmosphere). Thus, we assume that material released into the boundary layer becomes well mixed in this layer within a few time steps. Moreover, the assumption of complete mixing within the boundary layer is used in the DERMA model. In order to simulate a cold release at ground level, and following the assumption of complete mixing, all particles are emitted at equidistant heights from the surface to the top of the boundary layer. These particles are advected by the three-dimensional wind fields from the NWP model.

Turbulent Diffusion and Transport

DERMA is a dispersion model based on a multi-level puff parameterization (*Sørensen & Rasmussen, 1995; Sørensen, 1997*). A "puff" (i.e. a concentration field surrounding a particle) is associated with each particle adding up to the total concentration field. In the horizontal, a Gaussian distribution of the concentration is assumed for each puff. For puffs inside the boundary layer, an assumption of complete mixing is employed in the vertical, while for puffs above the boundary layer, a Gaussian distribution is employed.

For a puff p positioned at point (x_p,y_p,z_p) above the boundary layer ($z_p > h$), the Gaussian formula given by *Zannetti (1990)* is used. The height of the boundary layer (the mixing layer) is denoted by h. The puff contributes to the concentration field at the spatial location (x,y,z) with the amount C_p:

$$C_p = \frac{Q_p}{(2\pi)^{3/2}\sigma_y^2\sigma_z}\exp\left\{-\frac{1}{2}\left(\frac{x-x_p}{\sigma_y}\right)^2 - \frac{1}{2}\left(\frac{y-y_p}{\sigma_y}\right)^2\right\} \times\left(\exp\left\{-\frac{1}{2}\left(\frac{z-z_p}{\sigma_z}\right)^2\right\} + \exp\left\{-\frac{1}{2}\left(\frac{z+z_p}{\sigma_z}\right)^2\right\}\right), \tag{2}$$

where:

C_p – amount (mass) of tracer gas associated with the puff depending on the emission rate,

σ_y, σ_z - horizontal and vertical standard deviations of the spatial concentration distribution.

For a puff located within the boundary layer (i.e. for $z_p \le h$), we assume complete mixing in this layer, and therefore the following expression for the contribution to the total concentration field is used:

$$C_p = \frac{Q_p}{2\pi\sigma_y^2 h}\exp\left\{-\frac{1}{2}\left(\frac{x-x_p}{\sigma_y}\right)^2 - \frac{1}{2}\left(\frac{y-y_p}{\sigma_y}\right)^2\right\}\delta(z,h), \tag{3}$$

$$\delta(z,h) = \begin{cases} 1 & \text{for} \quad z \le h, \\ 0 & \text{for} \quad z > h. \end{cases} \tag{4}$$

From Gifford's random-force theory (*Gifford, 1984*) the following expression for the horizontal standard deviation is obtained:

$$\sigma_y^2 = 2K_y t_L\left\{\tau - (1-e^{-\tau}) - \frac{1}{2}(1-e^{-\tau})^2\right\}. \tag{5}$$

The parameter τ is the travel time, t, in units of the Lagrangian time scale, t_L, ($\tau = t/t_L$). For the simulations, we have used the value of the horizontal eddy diffusivity, K_y, of $6\cdot10^3$ m^2/s, and for the Lagrangian time scale, t_L, 10^4 s.

The expression above has the following asymptotic expressions:

$$\sigma_y^2 = \begin{cases} \frac{2}{3}K_y t_L^{-2} t^{-3} & \text{for} \quad t << t_L, \\ 2K_y t & \text{for} \quad t >> t_L. \end{cases} \tag{6}$$

The short-time asymptotic expression is derived also by *Smith (1968)* by assuming an exponential auto-correlation using the conditioned particle motion theory. The large-time asymptotic behaviour is the well known Fickian diffusion expression, which is also the limit of Taylor's statistical theory of diffusion.

The selected value of K_y for the horizontal eddy diffusivity was obtained by fitting results of DERMA using DMI-HIRLAM data to the official set of the ETEX tracer gas measurements (*Sørensen, 1998*). The horizontal and temporal resolutions of NWP data define an upper limit of the value of the horizontal eddy diffusivity mainly describing sub-grid scale diffusion.

For puff centres above the boundary layer, a Gaussian distribution is assumed for the vertical spatial distribution using the following expression for the standard deviation, σ_z:

$$\sigma_z^2 = 2K_z t_L\left\{\tau - (1-e^{-\tau}) - \frac{1}{2}(1-e^{-\tau})^2\right\} = \left(\frac{K_z}{K_y}\right)\sigma_y^2. \tag{7}$$

The height of the boundary layer is estimated by a bulk Richardson number approach (*Sørensen et al., 1996*). This approach is useful in cases where the vertical resolution of temperature and wind is limited as e.g. in output from NWP models. The bulk Richardson number, Ri_B, at height z above the ground surface is given by the following expression:

$$Ri_B = \frac{gz(\theta_v - \theta_s)}{\theta_s(u^2 + v^2)}, \tag{8}$$

where:

θ_s, θ_z - virtual potential temperature at the surface s and at the height z, respectively;

u, v - horizontal wind components at height z;

g - gravitational acceleration.

The top of the boundary layer is given by the height at which the bulk Richardson number reaches a critical value. This approach could be improved for the stably stratified boundary layer following *Zilitinkevich & Baklanov (2002)*.

Dry Deposition and Gravitational Settling

Dry deposition is the removal of gaseous and particulate nuclides or other pollutants from the atmosphere to the earth surface by vegetation or other biological or mechanical means. It plays an important role for most nuclides (excluding the noble gases).

For the DERMA model, it was included via the mass loss due to dry deposition in the calculation of source term Q_p - the amount of radionuclide associated with each puff p depending on the emission rate (the so-called source depletion method). As a first simple parameterisation of dry deposition we used a classic approach, based on the concept of the deposition velocity v_d. The dry deposition takes place in the lower surface layer and is not valid in the free troposphere ($z > h$).

Therefore, using the assumption employed in the DERMA model about complete vertical mixing within the atmospheric boundary layer (ABL) for each puff p, we can obtain the following simple formula for the mass loss due to dry deposition:

$$Q_p\big|_{n+1} = Q_p\big|_n \exp\left(-\frac{\Delta t \cdot v_d}{h}\right), \tag{9}$$

where:

Δt - time step of the model,

h - mixing layer height.

Prahm & Berkowicz (1978) showed that the source depletion method could give considerable errors of the surface air concentration in case of stable stratification of the ABL. If an air pollution model can simulate the vertical structure/profile of concentration within the ABL, especially for the local scale, the surface depletion approach is more suitable for simulation of dry deposition. However, in case of using the approach of complete vertical mixing within ABL (as it is done in the DERMA model), the difference between both methods is not significant. Calculation of the radionuclide amount deposited on the surface due to dry deposition is performed at each time step.

The dry deposition velocity depends on many parameters describing particles and characteristics of the ground surface and surface layer. For the simplest case of dry deposition parameterisation (in the emergency version of the DERMA model), we assume that the dry deposition velocity is constant for each nuclide and surface type (see Table 3.1.1).

However, it should be noted that this parameterisation is not very suitable for simulation of accidental releases, because numerous experimental studies (cf. e.g. an overview by *Baklanov & Sørensen (2001)*) showed that the dry deposition velocity depended on the size of the deposited

particles. Therefore, for the dry deposition velocity of more than 300 radionuclides the different values were used in the DERMA model.

Table 3.1.1. Maximum deposition velocities, $v_{d,max}$, (according to *Müller & Pröhl (1993)*).

Surface Type	**Maximum Deposition Velocity, $v_{d,max}$ (cm/s)**		
	Aerosol Radionuclides	*Elemental Iodine*	*Organic Iodine*
Soil	0.05	0.3	0.005
Grass	0.15	1.5	0.015
Trees	0.5	5	0.05
Other Plants	0.2	2	0.02

For particles, especially for heavy particles (radius r_p > 1 μm), the gravitational settling strongly affects the process of deposition to the surface. The effect of gravitational settling, described through the gravitation settling velocity, v_g, is included in the dry deposition velocity value. For particles with diameter of less than 4 μm, for which the airflow around the falling particle can be considered laminar, the gravitational settling velocity is given by Stokes' law (*Hinds, 1982*):

$$v_g = \frac{2C(\rho_p - \rho)gr_p^2}{9\nu}, \tag{10}$$

where:

ρ_p, ρ - particle and air densities, respectively,
g - gravitational acceleration,
r_p - particle radius,
ν - kinematic viscosity of air ($1.5 \cdot 10^{-5}$ m^2/s),
C - Cunningham correction factor (*Zanetti, 1990*), which for small particles (r_p < 0.5 μm) can be expressed:

$$C = 1 + \frac{\lambda}{r_p}\left[a_1 + a_2 \exp\left(-\frac{2a_3 r_p}{\lambda}\right)\right], \tag{11}$$

where:

λ - mean free path of air molecules (λ=$6.53 \cdot 10^{-5}$ m),
a_1=1.257, a_2=0.40, and a_3=0.55 - constants.

Wet Deposition

The Chernobyl accident has shown that the wet deposition or pollutant scavenging by precipitation processes is very important for evaluation of the radionuclide atmospheric transport from nuclear accidental releases as well as estimation of the deposited radioactivity pattern. Usually the wet deposition is treated in a standard way with a washout coefficient for the below-cloud scavenging and a rainout coefficient for the in-cloud scavenging (*Yamartino, 1985; Seinfeld, 1986; Zanetti, 1990*).

As a first approximation for the emergency response version of the DERMA model, for parameterisation of the wet deposition (absorption into droplets followed by droplet removal by

precipitation) of aerosol particles or highly soluble gases, we can describe the local rate of material removal as the first-order process:

$$\frac{dc}{dt} = \Lambda\left(r_p, x_i, t\right) \cdot c\left(x_i, t\right) \tag{12}$$

where:

$\Lambda(r_p, x_i, t)$ - total scavenging (washout or rainout) coefficient (depends on the height above the surface and on the time).

The wet deposition flux to the surface, in contrast to the dry deposition flux, is the sum of wet removal from all volume elements aloft, assuming that the scavenged material comes down as precipitation. For the DERMA model, by using the assumption of complete vertical mixing within the ABL and assuming that the rain clouds are contained in ABL, we can express the wet deposition velocity as:

$$v_w = \Lambda' \cdot H_r, \tag{13}$$

where:

Λ' - vertically averaged washout coefficient,

H_r - the height of the cloud base.

In case of simulation without splitting the scavenging process in washout and rainout, H_r will be the height of the cloud top. Thus, we obtain a formula similar to Eq. (9) for the calculation of the mass loss by the wet deposition:

$$Q_p\big|_{n+1} = Q_p\big|_n \exp\left(-\frac{\Delta t \cdot H_r \cdot \Lambda'}{h}\right). \tag{14}$$

If the height of the rain cloud base H_r is unknown, one can assume that $H_r = h$.

As it was mentioned above, the scavenging coefficient $\Lambda(r_p, x_i, t)$ includes the washout and rainout coefficients, and hence, it is possible to present it as a sum of two coefficients: $\Lambda(r_p, x_i, t) = \Lambda_w(r_p, x_i, t) + \Lambda_r(r_p, x_i, t)$. The washout and rainout mechanisms are spatially separated (the rainout is effective within the clouds, the washout below the clouds).

Washout

The below-cloud scavenging (washout) coefficient, Λ_w, for aerosol particles of radius r_p can be expressed in a general form as:

$$\Lambda_w = -\pi N_r \int a^2 w_a(a) E(r_p,a) f_a(a) da, \tag{15}$$

where:

N_r - total number of raindrops residing in a unit volume,

a - raindrop projected radius,

$E(r_p,a)$ - aerosol capture efficiency term,

$w_a(a)$ - vertical velocity of the raindrops (negative if downward),

$f_a(a)$ - probability-density function of the raindrop size distribution.

The limits of integration are from the ground surface to the cloud base. The aerosol capture efficiency $E(r_p,a)$ is a function of the radius of particle, r_p, and of rain drops, a, and depends upon several mechanisms mentioned by *Hales (1986)*:

- impaction of aerosol particles on the rain drop,
- interception of particles by the rain drop,
- Brownian motion of particles to the rain drop,
- nucleation of a water drop by the particle,

- electrical attraction,
- thermal attraction,
- diffusioforesis.

The washout coefficient, Λ_w, varies spatially and temporally. However, in order to simplify, one may use a vertically averaged washout coefficient, Λ_w', below the clouds in combination with the surface precipitation data.

As it is shown (*e.g. Baklanov, 1999*), in most models of long-range pollution transport the washout coefficient does not depend on particle radius. However, as it is mentioned in an overview by *Baklanov & Sørensen (2001)*, the $E(r_p,a)$ and correspondingly Λ_w strongly depend on the particle size (the so-called "Greenfield gap"). According to experimental data (*Tschiersch et al., 1995; Radke et al., 1977*), the washout coefficient for particle radii in the range of 0.01–0.5 μm is about of $0.1\cdot10^{-3}$–$0.5\cdot10^{-3}$ sec^{-1}, and it is two orders of magnitude smaller than that for particles larger than 4 μm.

Therefore, as a first approximation, *Baklanov & Sørensen (2001)* suggested a revised formulation of the vertically averaged washout coefficient for particles of different size:

$$\Lambda'(r_p,q)=\begin{cases} a_0\cdot q^{0.79} & \text{if} \quad r_p \le 1.4\ \mu\text{m} \\ \left(b_0+b_1 r_p+b_2 r_p^2+b_3 r_p^3\right) f(q) & \text{if} \quad 1.4\ \mu\text{m} < r_p < 10\ \mu\text{m} \\ f(q) & \text{if} \quad r_p \ge 10\ \mu\text{m} \end{cases}, \tag{16}$$

$$f(q)=a_1 q+a_2 q^2,$$

where:

q – precipitation rate (mm/h),

$a_0 = 8.4\cdot10^{-5}$, $a_1 = 2.7\cdot10^{-4}$, $a_2 = -3.618\cdot10^{-6}$,

$b_0 = -0.1483$, $b_1 = 0.3220133$, $b_2 = -3.0062\cdot10^{-2}$, and $b_3 = 9.34458\cdot10^{-4}$.

The effects of particle size and rain intensity on the washout coefficient, as calculated by the revised formulation (16) were analysed by *Baklanov & Sørensen (2001)* and it was shown that this formulation had a better correlation with the measurement data compared with the formulation of *Näslund & Holmström (1993)* and other formulations, which did not consider effects of the particle size.

Rainout

Beside washout below a cloud base, there are the following additional effects of wet deposition when air pollutants are transported inside clouds: 1) rainout between the cloud's base and top (scavenging within the cloud), and 2) wet deposition caused by deposition by fog. The first process of rainout between the cloud base and top depends on the types of precipitation (i.e. convective or dynamic types).

The rainout coefficient for the convective precipitation is more effective/intensive than the washout coefficient, and it can be estimated (according to *Maryon et al. (1996)*) by the following formula:

$$\Lambda_r'(r_p,q) = a_0\, q^{0.79}, \tag{17}$$

where: $a_0 = 3.36\cdot10^{-4}$. *Crandall et al. (1973)* showed simulations of different mechanisms for rainout in which the rainout coefficient was not a strong function of the particle size.

The rainout coefficient for the dynamic precipitation is approximately equal to the washout coefficient, and hence, the rainout effect in this case can be also estimated by Eq. (16).

Snow Scavenging

According to recent publications (e.g. *Hongisto, 1998; Maryon & Ryall, 1996*) in most models the processes of scavenging by snow are described by the same formulae as for rain (e.g. Eqs. (14), (16), and (17) in our case), but with other values of the scavenging coefficient, Λ. The values of Λ for snow are 2–10 times lower than the washout coefficient for rain with equivalent precipitation rates.

For scavenging by snow (according to *Maryon et al. (1996)*), the following simple formulation without any dependence of the coefficient Λ' on the particle radius could be used:

$$\Lambda_s'(q) = a_0 q^b, \tag{18}$$

where: $a_0 = 8.0 \cdot 10^{-5}$ and $b = 0.305$ for scavenging by snow below the cloud base and between the cloud base and top for dynamic precipitation; and $a_0 = 3.36 \cdot 10^{-4}$ and $b = 0.79$ for scavenging by snow between the cloud base and top for convective precipitation.

Unfortunately, the processes of scavenging by snow are not well studied. For example, there are effects of the water content in snowflakes on the scavenging by snow, especially for the air temperatures close to 0°C (*Karlsson & Nyholm, 1998*), but there is no relevant experimental data for this effect.

Radioactive Decay

Radioactive decay transforms many basic dose contributing nuclides and should be taken into consideration for simulation of the possible radioactive contamination. The decay effects in the following ways:

- simple decay to non-radioactive elements;
- radioactive daughter nuclides (B, or B1, B2);
- secondary decay of daughter nuclides (C, D, etc.).

It is possible to split the DERMA modelling of the radioactive decay into two basic phases. The first phase is employed during the airborne transport of the short-living nuclides (like ^{131}I). The second phase is employed after the airborne transport has been completed and the long-living nuclides (like ^{137}Cs) have been deposited to the ground surface. This phase could be done in a separate subprogram/ submodel.

For ^{131}I, the simulation of physical and chemical form of nuclides includes three forms of iodine: gaseous forms - elemental iodine and organic iodine (e.g., CH_3I), aerosol form – iodine attached to aerosol particles. During the first week, the gaseous forms of ^{131}I dominate. The dry deposition velocity, v_d, is corrected/ recalculated for 70% of gaseous ^{131}I, and for the rest of the particles it is almost equal to v_d of SO_4 particles.

The radioactive decay is taken into account through mother (A) and possible daughter nuclides (B, C, etc.) by the following formulae:

$$\begin{aligned} \frac{dA}{dt} &= -\lambda_a A, \\ \frac{dB}{dt} &= -\lambda_b B + \lambda_a A, \\ \frac{dC}{dt} &= -\lambda_c C + \lambda_b B, \end{aligned} \tag{19}$$

where λ_a, λ_b, and λ_c are the decay constants for corresponding nuclides.

At the current stage, only the simple decay of radionuclides is included into the DERMA model simulation.

3.2. *METEOROLOGICAL DATA FOR DISPERSION MODELLING*

The Danish Meteorological Institute provides meteorological and related services within the large geographical area of the Kingdom of Denmark (Denmark, the Faeroe Islands, and Greenland), including surrounding waters and airspace, as well as global services.

In our study, we considered two types of the gridded datasets as input data. They are the DMI-HIRLAM and **ECMWF** (**E**uropean **C**entre for **M**edium-Range **W**eather **F**orecast) datasets. Both datasets were used for the dispersion modelling purposes. The DMI-HIRLAM dataset was used to model atmospheric transport, dispersion, and deposition only of ^{137}Cs for all 16 NRSs during the period studied (Oct 2001 - Nov 2002). The ECMWF dataset was used to model atmospheric transport, dispersion, and deposition for three radionuclides - ^{137}Cs, ^{131}I, and ^{90}Sr – but only from one NRS (Leningrad NPP). The model runs based on different types of datasets were performed for comparison purposes, and first of all, to compare the accuracy of the wet deposition patterns. For the specific case studies, the DMI-HIRLAM dataset was used. The description of these gridded datasets is given below.

It should be noted that in this study, the SGI Origin scalar server was used for DERMA runs and the NEC SX6 supercomputer system (http://www.ess.nec.de) of DMI was used for DMI-HIRLAM modelling computational purposes, and all modelled data were stored on the DMI UniTree mass-storage device as well as recorded on CDs.

DMI-HIRLAM Datasets

The DMI-HIRLAM high-resolution meteorological data (Figure 3.3.1b: D-version: 0.05°, N- and E-versions: 0.15° or G-version: 0.45°, with 1 hour time resolution) are used as input data for high-resolution trajectory or dispersion simulations. The vertical model levels (31 levels in total presently, and 40 levels from December 2002) are presently located at 33, 106, 188, 308, etc. meters for a standard atmosphere. The High Resolution Limit Area (HIRLAM) numerical weather prediction model has been run operationally by DMI (http://www.dmi.dk) for the European territory and for the Arctic region since the late 1980s. But it can be run also, after extending the grid domain, for other geographical regions. The DMI 3D Lagrangian trajectory model (*Sørensen et al., 1994*) calculates forward and backward trajectories for any point in the area of interest. It can utilize meteorological data from the different versions of DMI-HIRLAM as well as the ECMWF global model. The present DMI weather forecasting system is based on HIRLAM 4.7 (*Sass et al., 2000*). The forecast model is a grid point model. The data assimilation is intermittent and based on the 3-D variation data assimilation (3DVAR) scheme.

The operational system consists of four nested models called DMI-HIRLAM-G, -N, -E, and -D. These models are identical except for horizontal resolutions and integration domains. The model domains are shown in Figure 3.1.1 (left block) or Figure 3.3.1b. The lateral boundary values for the "G" model are ECMWF forecasts, while those for "N" and "E" are "G" forecasts, and those for the "D" model are "E" forecasts. For some limited periods of time the DMI-HIRLAM system was run for other areas as well, e.g. for China, Afghanistan and surrounding regions.

The forecasting system is run on the NEC-SX6 supercomputer. The DMI-HIRLAM data can be used in the operational mode or from the archives.

ECMWF Dataset

The meteorological data from the European Centre for Medium-Range Weather Forecasts (ECMWF), Reading, UK are based on the ECMWF's global model forecasts and analyses (http://www.ecmwf.int) having a resolution up to 0.5° × 0.5° latitude vs. longitude and 3 hours time interval for both Northern and Southern hemispheres. It consists of the geopotential, temperature,

vertical velocity, u and v components of horizontal wind, relative humidity and specific humidity at each level, etc. Analysis has been done on a daily basis at 00, 06, 12 and 18 UTC terms.

The ECMWF has the following data archives: ECMWF/WCRP level III-A Global Atmospheric Data Archive (TOGA), Operational Atmospheric Model, ERA-15 (ECMWF Re-Analysis 15), ERA- 40 (ECMWF Re-Analysis 40), Wave Model, Ensemble Prediction System (EPS), Seasonal Forecast, and Monthly Means.

The ERA-15 production system generated re-analyses from December 1978 to February 1994. The ERA-15 Archive contains global analyses and short range forecasts of all relevant weather parameters, beginning with 1979, the year of the First GARP Global Experiment (FGGE). The Level III-B archive is subdivided into three classes of data sets: Basic 2.5° x 2.5° Data Sets (17 vertical pressure levels); Full Resolution Data Sets (e.g. 1° x 1°, 31 hybrid model vertical levels); Wave archive.

The data sets are based on quantities analysed or computed within the ERA-15 data assimilation scheme or from forecasts based on these analyses. The Basic Data Sets contain values in a compact form at a coarse resolution. They are particularly suitable for users with limited data processing resources. The Full Resolution Data Sets provide access to most of the data from the ERA-15 atmospheric model archived at ECMWF. These archives have a higher space resolution. They should only be used where high resolution is essential; in this respect they are particularly suited for use in conjunction with case studies and as initial conditions for high-resolution models. This archive includes analysis, forecast accumulation and forecast data. Data are available on the surface, pressure levels and model levels.

The new reanalysis project ERA-40 (*Simmons and Gibson, 2000*) will cover the period from mid-1957 to 2001 overlapping the earlier ECMWF reanalysis, ERA-15, 1979-1993. Analysis and forecast fields will only be made available as complete years and only after validation.

In this particular study we used ECMWF data, available at DMI for the forecast mode or analysed and archived mode. The horizontal resolutions of the meteorological data are different from year to year. For example, for the year 2000 the data have a resolution of 1° x 1° latitude vs. longitude and 6 hours time resolution. It consists of temperature, u and v components of horizontal wind, and specific humidity at each level, plus surface fields. Analyses have been done at 00 and 12 UTC.

3.3. *LONG-TERM DISPERSION MODELLING APPROACH*

In previous project reports (e.g. *Baklanov et al., 2002; Baklanov and Mahura, 2001; Mahura and Baklanov, 2002*) we used for the probabilistic risk analysis trajectory models only, and the DERMA model or some other dispersion models were used for separate case studies or for operational forecast of possible accidental release transport (e.g. *Sørensen et al., 1998; Baklanov, 1999, 2000; Baklanov and Sørensen, 2001*).

The long-term dispersion modelling approach, suggested in this study, is another useful tool for the risk assessment methodology. For this purpose, the long-range transport model DERMA (see §3.1) is employed in a long-term simulation mode, described in this chapter. It means the simulation for a time period not shorter than one year (it could be months or seasons for some purposes as well) with a continuous or discrete periodical release from a NRS. As input data, the model can use meteorological operational forecast or archived analysed data from the DMI-HIRLAM limited area model or the ECMWF global model (see § 3.2). The DERMA model can simulate radionuclide atmospheric transport, dispersion, and deposition for atmospheric releases of radioactivity occurring at the selected geographical locations.

The approach suggested for the long-term dispersion modelling has several important points and peculiarities depending on the particular study problem and the type of models used. They include:

(i) type and parameters of release (continuous, discrete, periodical; different height, etc);
(ii) time range for simulations: time limit for plume transport (e.g., three, five or ten days) and total study period (e.g., one, two, five, eleven or more years);
(iii) nuclides of main interest and their particle size distributions;
(iv) calculation of the further radioactive decay of deposited nuclei taking place after the end of the simulation period (for long-term consequence studies).

The main peculiarities for the Eulerian and Lagrangian types of models are important for the choice of the release type and the time range for simulations. In general, Lagrangian models involve shorter computation time, which is due to the fact that Eulerian models perform calculations in every grid cell of the model atmosphere whereas Lagrangian models confine calculations to the limited volume of the plume. Regarding the advection properties of the two kinds of models, Eulerian models need to use advanced and computationally expensive methods whereas Lagrangian models are inherently accurate. Besides, Eulerian models respond to singularities such as a point source by creating numerical noise, which is not the case for Lagrangian models. In case of a Lagrangian model the time limit for plume (or particle) transport (e.g., two, three, five or ten days) is an important parameter due to the depending calculation expenses. It can be controlled in the model by excluding further consideration of puffs leaving the study area or puffs reaching a lowest limit of concentration. In our studies by the Lagrangian model of DERMA we found that the chosen limitation of puff modelling by 5–6 days after the release ended is quite suitable, as the contaminated cloud in general has left the area of interest (30°N–90°N vs. 60°W–135°E, see Figure 3.3.1a) within this time period. For Eulerian models one does not need to care about the life-time of airborne release and to limit the simulation time for each released portion. Besides, the choice of the release type (continuous or discrete) does not affect the computation time in Eulerian models.

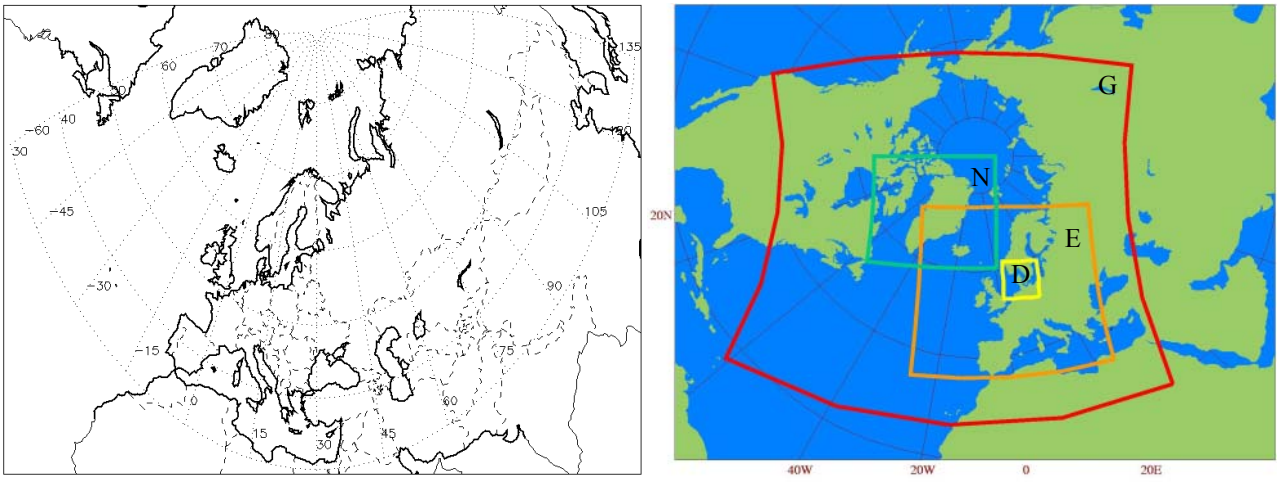

a **b**

Figure 3.3.1. Domain of recalculated dispersion modelling fields (a) and the areas covered by the various DMI-HIRLAM versions (b).

The release height can be also an important parameter. However, previous sensitivity studies (*Bergman et al., 1998; Baklanov et al., 2001*) showed that variations of the initial plume rise (release height) below the mixing height only slightly affected the results outside the local scale,

while plume rise above that level led to radically changed patterns with relatively little depositions on the local and meso-scale ranges. Thus, a release into the PBL in comparison with a release to the free troposphere leads to large differences in the deposition patterns and the lifetimes of radionuclides in the atmosphere (a week or more in the second case). However, considering that most accidental releases from NRSs initially rise to not more than 700 meters, for this long-term dispersion modelling study we can simplify the simulations by considering a continuous "unit discrete hypothetical release" (UDHR) into the PBL.

The suggested approach for long-term modelling can be realised practically by the following ways of using NWP data: (i) simulations from meteorological data archives, (ii) every day real-time runs using analysed NWP model data available in the NWP database followed by archiving of the dispersion simulation data. Certain national meteorological services, e.g. SMHI, perform daily forecasting of atmospheric dispersion from hypothetical accidental releases from a number of NPPs. Such data could be archived for long-term statistical risk analyses. However, the quality will be lower than for the results based on analysed NWP data.

The simulated fields of the air contamination and deposition on the surface by this approach of the long-term dispersion modelling can be used and interpreted as:

(i) long-term effects (accumulated or average contamination) of existing continuous release sources (ventilation emission from NRSs (e.g., ^{129}I from Sellafield, noble gases from NPPs), natural radioactivity emission (e.g., Rn products), industrial pollution etc.);
(ii) probabilistic characteristics of possible radioactive contamination of different territories in case of an accident at an NRS.

For this particular study of the Arctic Risk project, we followed several basic assumptions in practical simulations.

First, for simplicity, for all 16 NRSs we selected the continuous "unit discrete hypothetical release" (UDHR) of radioactivity ($1 \cdot 10^{10}$ Bq/s) with discrete emitting of puffs (every 60 minutes) during 24 hours. Hence, in this case the total amount of radioactivity released during one-day is equal to $8.64 \cdot 10^{14}$ Bq.

Second, we considered only one radionuclide ^{137}Cs, as a radionuclide of key importance. However, the calculation might be done for any of more than 300 radionuclides incorporated into the database of the DERMA model. In particular, for the specific case studies - ^{131}I and ^{90}Sr were considered additionally. For one NRS (Leningrad NPP) these two radionuclides were also used for one year simulation. Simulation for many nuclides requests longer computing time. However, the computation time is not proportional to the number of nuclides considered. Run times for DERMA simulations as a function of the number of simultaneously handled nuclides are presented in Figure 3.3.2. The example simulations involved 66 hours integration corresponding to a 6-hours release and made use of DMI-HIRLAM-G NWP model data.

Third, the simulation was performed during one year (October 2001–November 2002) on a daily basis considering the length of the 5-day trajectories (i.e. after release of radioactivity occurred from the site, the tracking of the radionuclide cloud was limited to 5 days of atmospheric transport from each site). The DERMA model was run daily (between 2–6 a.m.) on the DMI computer system. Daily, after each run, the dispersion modelling results were compressed, and then archived on the DMI UniTree mass storage system (as the first backup of data). Moreover, twice per month they were also recorded on CDs (as the second backup of data). The directory size of each daily run varies between 25 and 50 Mb, and hence, it will be around 1200 Mb per month.

Fourth, to minimize the computing resources used for the dispersion modelling approach, in our study we selected only one year, although it should be noted that for the statistical analysis the multiyear period is more preferred.

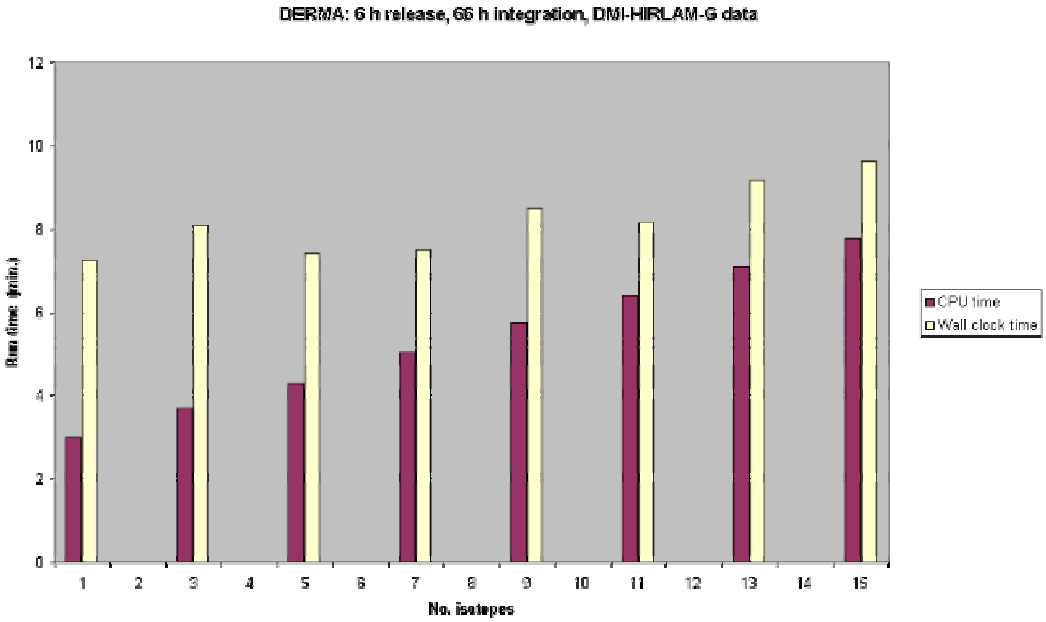

Figure 3.3.2. Run times for DERMA simulations as a function of the number of simultaneously handled nuclides. The simulations involved 66 hours integration corresponding to a 6-hours release and made use of DMI-HIRLAM-G model data.

Firth, using the DERMA model, we calculated several important characteristics. Among these characteristics are the following:

- air concentration (Bq/m^3) of the radionuclide in the surface layer – **surface air concentration** field,
- time-integrated air concentration (Bq·h/m^3) of the radionuclide in the surface layer – **integral air concentration at surface** field,
- dry deposition (Bq/m^2) of the radionuclide on the underlying surface – **dry deposition** field, and
- wet deposition (Bq/m^2) of the radionuclide on the underlying surface – **wet deposition** field.

Sixth, as input data for the DERMA model run, the meteorological fields simulated by the DMI-HIRLAM model were used when modelling for ^{137}Cs was done for 16 NRSs. As input data in a separate run of the DERMA model the ECMWF meteorological fields were used when modelling for all three radionuclides - ^{137}Cs, ^{131}I, and ^{90}Sr - was done for the Leningrad NPP. The output fields for all characteristics were recorded in separate output files every 3 hours of atmospheric transport starting from the moment of release.

Additionally, it should be noted that the total deposition field for the radionuclide can be calculated as a sum of dry and wet deposition fields. All these calculated characteristics can be represented by two-dimensional fields where the value of the calculated characteristic is given in the latitude-longitude grids of the model grid domain. The areas covered by the various DMI-HIRLAM versions can be seen in Figure 3.3.1b. For the ECMWF data available, the domain covers nearly the entire Northern Hemisphere, i.e. extending between 12˚N–90˚N vs. 180˚W–180˚E.

From this grid domain, we extracted and incorporated data into the new grid domain in the region of interest (Figure 3.3.1a), which covers territories of the North Atlantic and Arctic Oceans, and Eurasian continent (30-89˚N vs. 60˚W-135˚E). This new domain had a resolution of 0.5˚ vs.

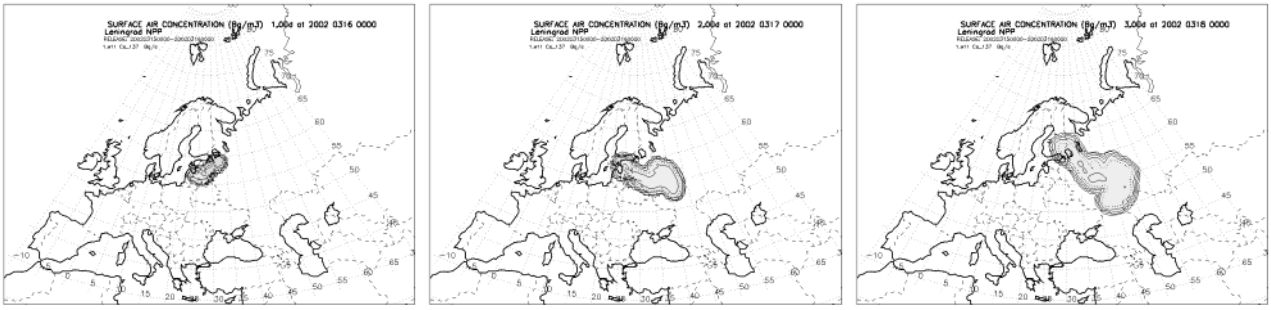

1.0 day 2.0 days 3.0 days

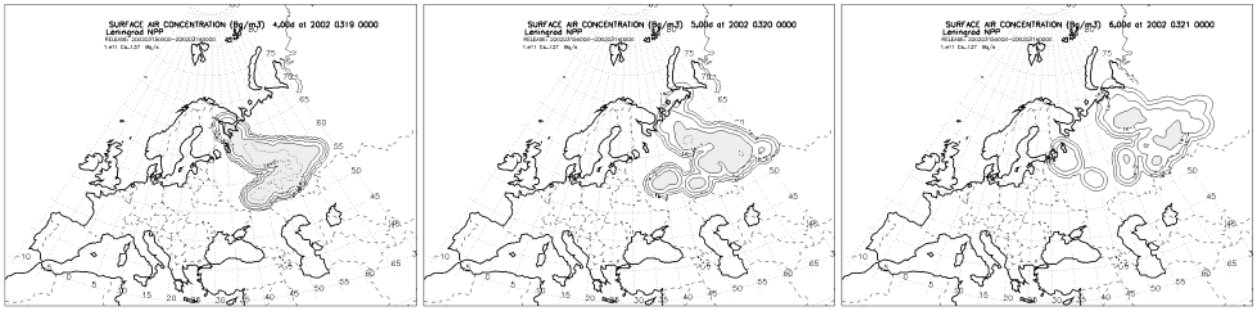

4.0 days 5.0 days 6.0 days

Figure 3.3.3. Temporal variation of the Cs^{137} surface air concentration for the "unit discrete hypothetical release" occurred at the Leningrad NPP during 15 -16 Mar, 2002, 00 UTC.

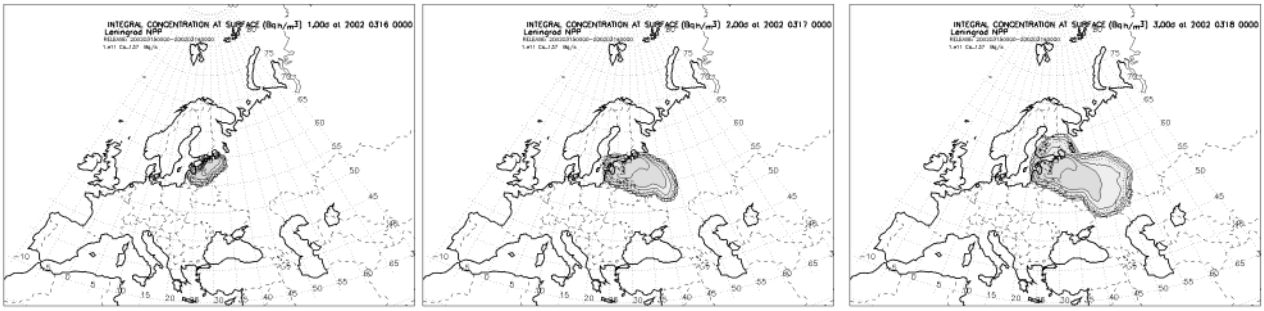

1.0 day 2.0 days 3.0 days

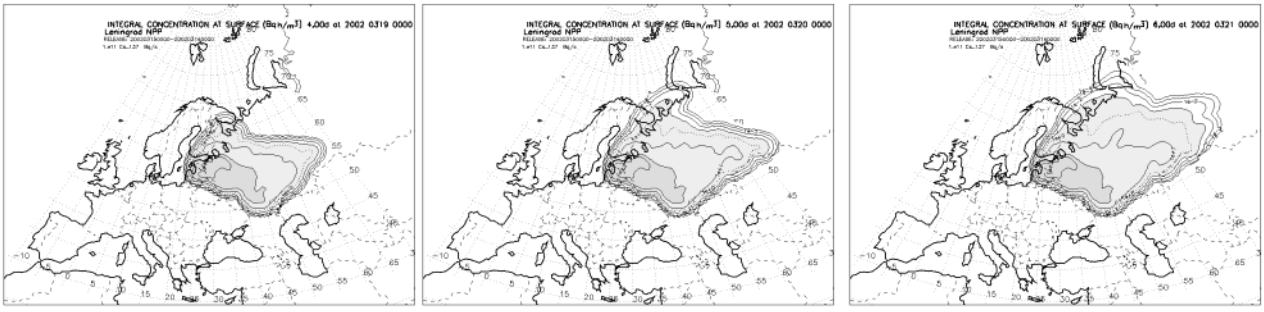

4.0 days 5.0 days 6.0 days

Figure 3.3.4. Temporal variation of the Cs^{137} integral concentration at surface for the "unit discrete hypothetical release" occurred at the Leningrad NPP during 15 -16 Mar, 2002, 00 UTC.

0.5˚ of latitude vs. longitude. It consisted of 391 vs. 119 grid points along longitude vs. latitude. To save storage space, the recalculated fields were re-recorded every 6 hours instead of original 3 hour intervals. Moreover, because of missing data in the archives and processing problems, we did not calculate fields for a few percent for some days during the October 2001 – November 2002 in the HIRLAM dataset.

Examples of the dispersion modelling for a particular date of release for several NRSs in the Euro-Arctic region are shown in Figures 3.3.3-3.3.5. Figure 3.3.3 shows the surface air concentration (Bq/m^3) of ^{137}Cs within the surface layer of atmosphere after the "unit discrete hypothetical release" at the Leningrad NPP occurred during 15 Mar, 00 UTC - 16 Mar, 00 UTC, 2002. As we see (on a daily basis), as the radioactive cloud propagates from the NRS location, the concentration decreases as expected, in general, with distance increasing from the source.

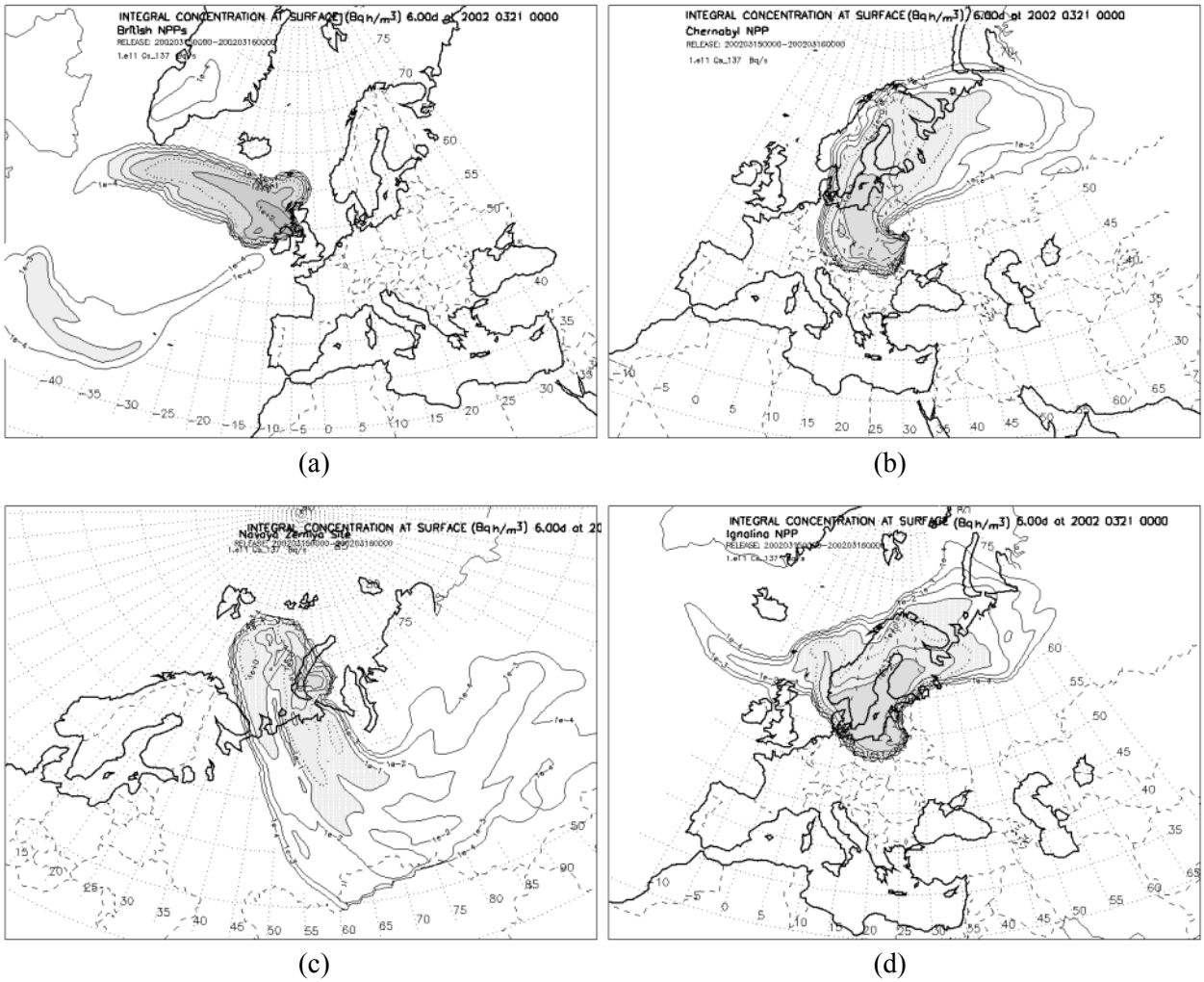

Figure 3.3.5. Cs^{137} integral concentration at surface after 6 days of the "unit discrete hypothetical release" occurred during 15 -16 Mar, 2002, 00 UTC at the a) Block of the British NPPs, b) Chernobyl NPP, c) Novaya Zemlya test site, and d) Ignalina NPP.

Figure 3.3.4 shows the integral air concentration (Bq·h /m^3) of ^{137}Cs at the surface after the same UDHR at the Leningrad NPP occurred during the same day. The integral air concentration is represented by a sum of air concentrations integrated over time through the fields at the subsequent temporal steps. Therefore, we see the accumulating concentration of ^{137}Cs at various temporal steps where the area closer to NRS has the higher magnitudes compared to remote areas from the site.

Figure 3.3.5 shows the integral concentration of Cs^{137} at surface after 6 days of the "unit discrete hypothetical release" occurred at NRSs during 15 -16 Mar, 2002, 00 UTC. The Figure 3.3.5a shows initially atmospheric transport of the contaminated cloud in the western direction from the block of the British NPPs toward the North Atlantic region. Further, during several days it moved anticlockwise reaching the British Islands. The integral concentration has the highest magnitude in vicinity of the British Islands, and it decreases significantly as the contaminated cloud passing over the ocean. The Figure 3.3.5b shows atmospheric transport from the Chernobyl NPP initially in the north-eastern direction from the site, and later the contaminated cloud is transported by westerlies.

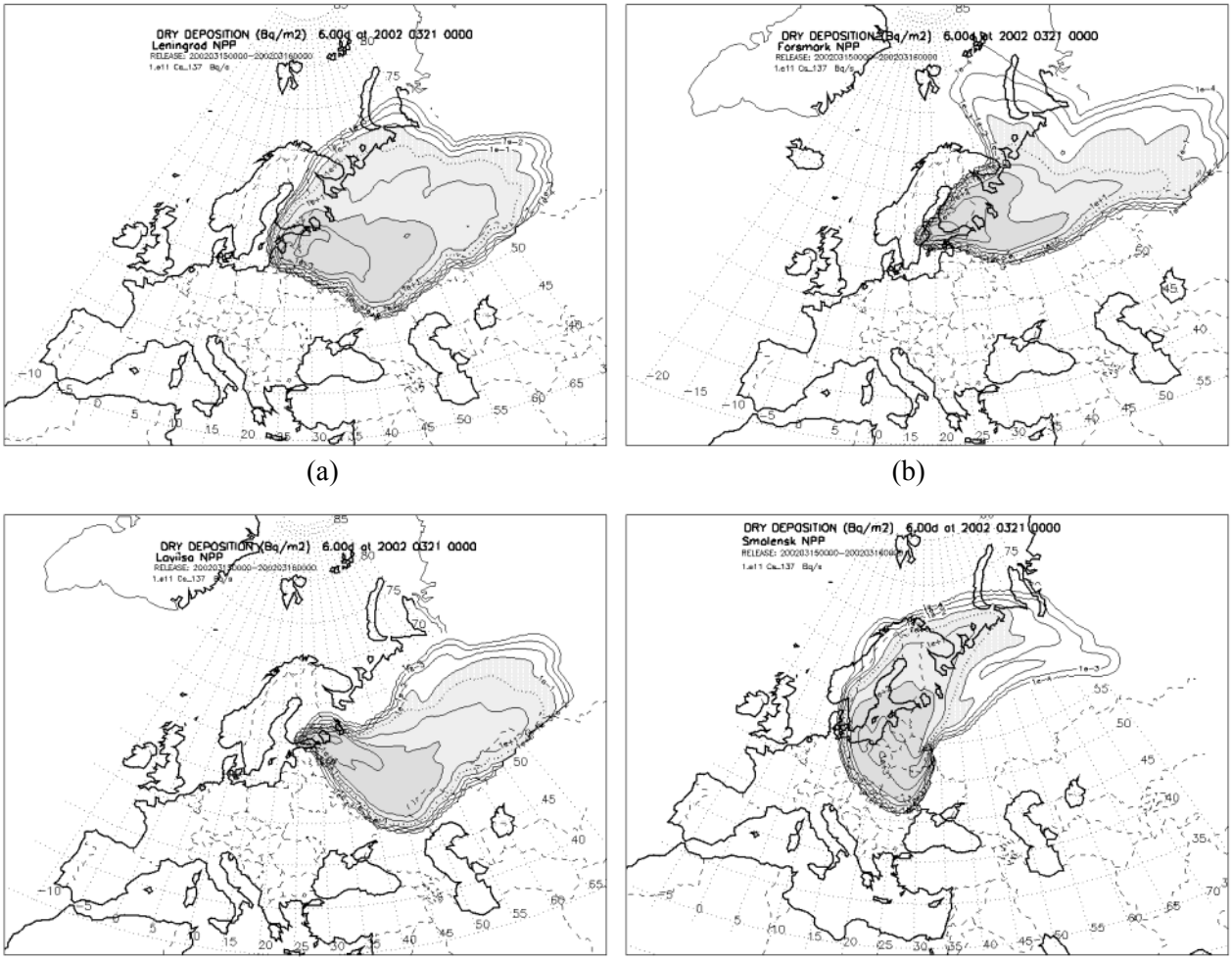

Figure 3.3.6. Cs^{137} dry deposition field after 6 days of the "unit discrete hypothetical release" occurred during 15 -16 Mar, 2002, 00 UTC at the a) Leningrad NPP, b) Forshmark NPP, c) Loviisa NPP, and d) Smolensk NPP.

Figure 3.3.5c shows that the contaminated cloud originated over the Novaya Zemlya Archipelago travelled initially over the Barents and Kara Seas, and then passed over the large areas of the Russian Arctic territories in the southern direction arriving to Siberia with westerlies. It even reaches the northern borders of Kazakhstan. The "sharp cut" off the cloud over this region is related to a limitation of the G-version of the DMI-HIRLAM model. Figure 3.3.5d similarly to the previous figures shows a distribution of the integral air concentration at the end of the six day of atmospheric transport from the Ignalina NPP. There it can be seen that the contaminated air mass was transported in both eastern and north-western directions from the site passing over the Baltic States, Nordic countries, Poland, Byelorussia, Northwest Russia and aquatorias of the North Atlantic and Arctic seas.

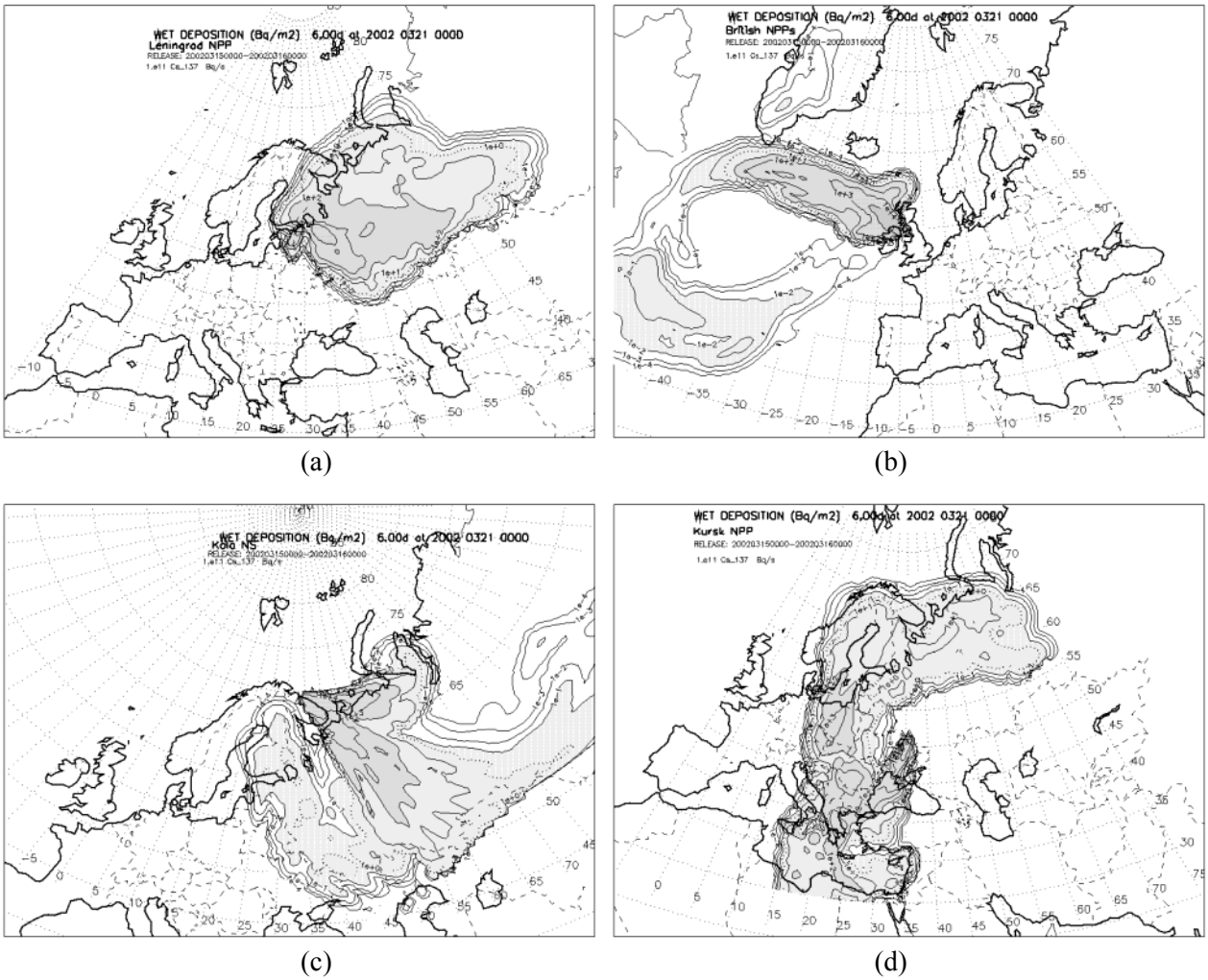

(a) (b)

(c) (d)

Figure 3.3.7. Cs^{137} wet deposition field after 6 days of the "unit discrete hypothetical release" occurred during 15 -16 Mar, 2002, 00 UTC at the a) Leningrad NPP, b) Block of the British NPPs, c) Kola Nuclear Submarine site, and d) Kursk NPP.

The dry deposition fields for ^{137}Cs (Bq/m^2) after the same release occurred during 15-16 Mar 2002, 00 UTC is shown in Figure 3.3.6. It should be noted that for the Leningrad NPP (as for any other selected site) the structure of the dry deposition field (Figure 3.3.6a) resembles the structure of the integral air concentration field (see Figure 3.3.4, at 6.0 days). Other examples of the dry

deposition fields – for the Forshmark, Loviisa, and Smolensk NPPs – are shown in figures b, c, and d, respectively. For all these fields the highest dry deposition is observed in vicinity of the sites and decreases as the contaminated cloud propagates from the sites.

The examples of the wet deposition fields for ^{137}Cs (Bq/m^2) for the same release are shown in Figure 3.3.7. The structure of the wet deposition fields is different due to the contribution of the wet removal processes (e.g. washout and rainout by precipitation) during the radionuclide atmospheric transport. It has a "spotted" nature, i.e. we observe the higher values of the wet deposition at the surface where precipitation occurred.

IV. METHODOLOGY FOR ANALYSIS OF DISPERSION MODELLING RESULTS

In this chapter, we will focus on further use of the dispersion modelling results, e.g. their representation in form of various indicator fields (§4.1), applicability for the calculation of doses for population groups due to food chains, etc. (§4.2), as well as applicability for the risk assessment using GIS technology (§4.3).

4.1. *PROBABILISTIC ANALYSIS FOR DISPERSION MODELLING RESULTS*

The dispersion modelling results might be analysed in a similar manner (*Baklanov & Mahura, 2001; Mahura & Baklanov, 2002*) to those for the trajectory modelling results. Further, we analyze the following: integral concentration at surface, dry deposition and wet deposition patterns of radionuclide. Let us consider two approaches to construct probability fields for each of these characteristics. It should be noted that in both approaches for calculation of fields, only data with "valid dates" were used (i.e. when original meteorological data were available for computation, and the dispersion simulation was performed without any computational problems).

All characteristic values are given in a gridded domain having $M_{lat} \times M_{lon}$ latitude vs. longitude (391 vs. 119) grid points with a size of $\Delta Y \times \Delta X$ degrees (0.5º x 0.5º) latitude vs. longitude for each day during October 2001 – November 2002. As an example, we select only one characteristic - integral air concentration of radionuclide, although similar steps in the construction of fields could be applied for all the other characteristics – dry, wet, and total deposition.

The **first approach** to construct fields based on the results of dispersion modelling (an example is shown in Figure 4.1.1a) considers the distribution of the total sum of daily continuous discrete releases of radioactivity at the site during the time period of interest (for instance: month, season, or year). Let's call this field the **summary field** for one of the chosen characteristics, and note that it is a field integrated over a considered period.

For example, for integral air concentration, at any grid point - (i,j) - the total sum ($C_{i,j}$) is equal to the sum of integral air concentrations (c_{ijk}) at the end of the 6th day of atmospheric transport from the site for each daily release of radioactivity during the period of interest:

$$C_{i,j} = \sum_{k=1}^{TP} c_{ijk},$$

$$i = 1, M_{lon}, \qquad j = 1, M_{lat},$$

where:

TP – the number of valid dates in the selected time period of interest,

M_{lat}, M_{lon} - the number of the domain grid points along latitude (119) and longitude (391),

i,j – the grid point in the gridded domain,

c_{ijk} – the integral air concentration in the grid point i,j of the gridded domain at the end of the 6th day of atmospheric transport due to one day release of radioactivity at the site during k day within the period of interest,

$C_{i,j}$ - the summary integral air concentration in the grid point i,j of the gridded domain at the end of the 6th day of atmospheric transport due to one day releases of radioactivity at the site during all days ($k = 1,TP$ days) within the period of interest.

This type of field shows the most probable geographical distribution of the radionuclide integral air concentration at the surface if the release of radioactivity occurred during the period of interest.

The **second approach** to construct fields (an example is shown in Figure 4.1.1b) is simply based on calculating the average value from the summary field obtained in the first approach. Let's call this field the **average field** for one of the chosen characteristics. In this case, we divide the calculated summary field values ($C_{i,j}$) in grids by the valid number (*TP*) of days during the selected period of interest.

$$C_{i,j} = \frac{\sum_{k=1}^{TP} c_{ijk}}{TP},$$

$$i = 1, M_{lon}, \qquad j = 1, M_{lat}.$$

This type of field shows the most probable averaged distribution of the radionuclide integral air concentration at the surface when the release of radioactivity occurres during one average day within the period of interest.

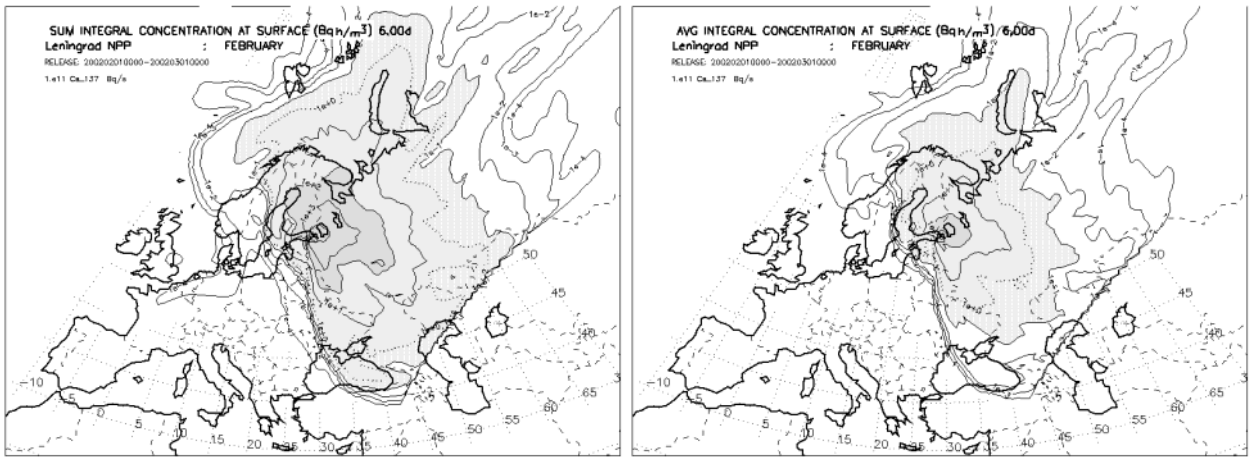

(a) (b)

Figure 4.1.1. Cs^{137} summary (a) and averaged (b) integral concentration at surface fields as a result of the "unit discrete hypothetical release" occurred during 1 Feb – 1 Mar, 2002, 00 UTC at the Leningrad NPP.

It should be noted, that for convenience of comparison the temporal variability in characteristic patterns (between months or seasons) can be underlined by isolines at similar intervals, although every field could be reconstructed with different threshold orders of magnitude than those selected.

Similarly, the summary and average fields may be calculated for the wet and dry deposition patterns. Examples of these fields are shown in Figures 4.1.2 and 4.1.3. Moreover, the total deposition fields (summary and average) could be calculated by summing the summary and average dry and wet deposition fields, respectively.

Some important comments should be also taken into account.

First, it should be noted that using average and summary fields it is possible to interpolate data to a particular geographical area of interest (enclosed by geographical boundaries) or for a particular geographical location (for example, a city).

Second, the summary fields might be used further to calculate doses accumulated over the considered period (month, season, year) – i.e. monthly doses, seasonal doses, or annual doses. These summary fields will be more representative if the routine discharges of radioactivity from NRS are considered.

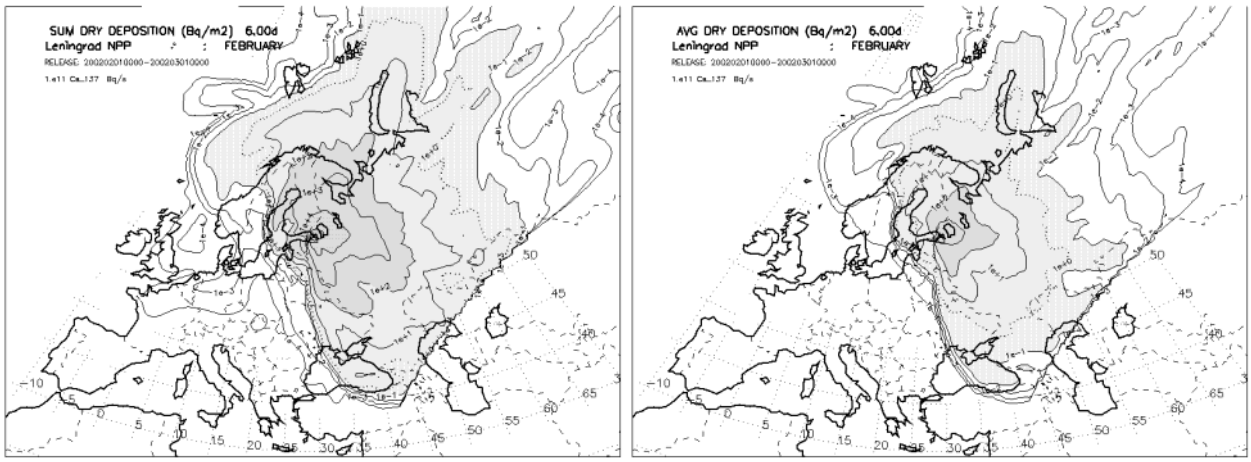

(a) (b)

Figure 4.1.2. Cs^{137} summary (a) and averaged (b) dry deposition fields as a result of the "unit discrete hypothetical release" occurred during 1 Feb – 1 Mar, 2002, 00 UTC at the Leningrad NPP.

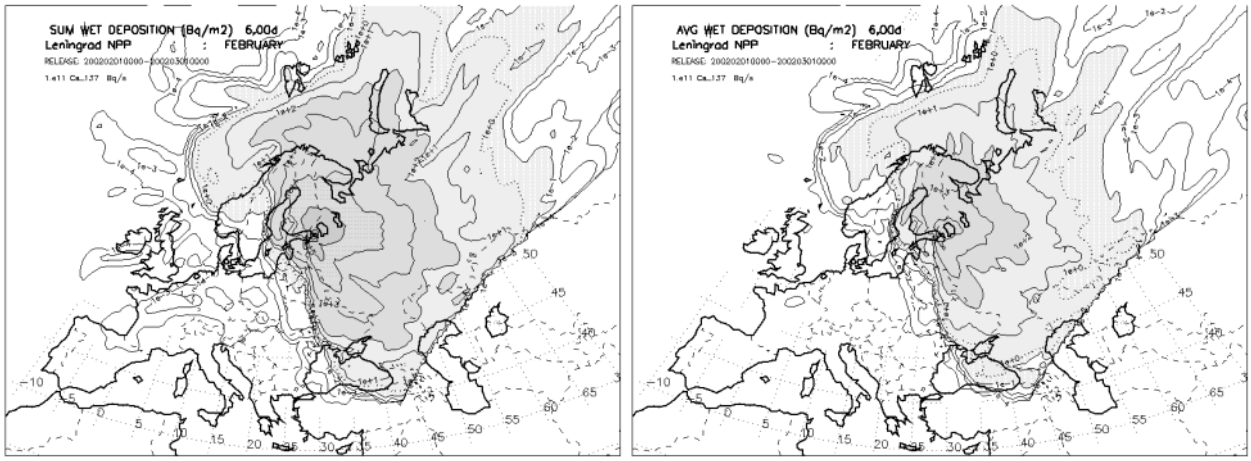

(a) (b)

Figure 4.1.3. Cs^{137} summary (a) and averaged (b) wet deposition fields as a result of the "unit discrete hypothetical release" occurred during 1 Feb – 1 Mar, 2002, 00 UTC at the Leningrad NPP.

Third, the average fields of these characteristics might be used further to calculate doses accumulated during one day averaged over the considered period (month, season, and year) – i.e. average daily doses for a particular month, season, or year. These average fields will be more representative if the accidental short-term releases of radioactivity from NRS are considered.

Fourth, of course, the summary fields of characteristics will have the larger areas enclosed by the isolines as well as the order of characteristic magnitudes will be higher in comparison with the average fields.

Fifth, because all the fields were calculated for the unit hypothetical release, it is possible to recalculate or rescale these fields for another accidental release of radioactivity at different magnitude rates.

Sixth, in calculating atmospheric transport and deposition of radioactivity releases (with a duration of one day) at NRSs, we limited our calculation to 5 days after the release end at the site. As uncertainties in the modelling of atmospheric transport after 5 days became too large, the calculated fields for a one-day release were assumed to be unchangeable, i.e. we did not apply any loss processes after that term. Hence, once material was deposited to the surface there is no radioactive decay.

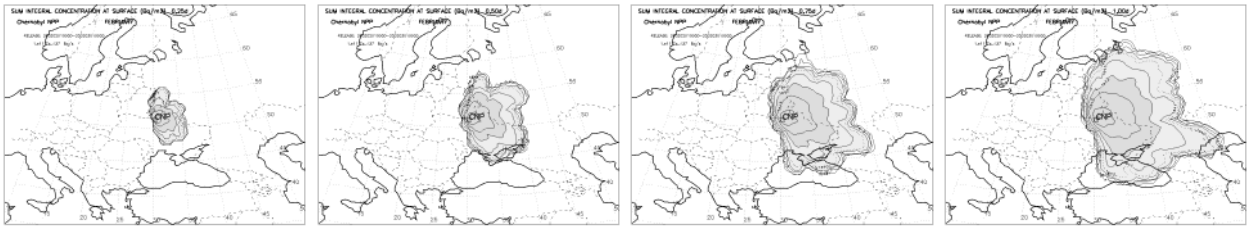

(a) (b) (c) (d)

Figure 4.1.4. Cs^{137} summary integral concentration at surface fields as a result of the "unit hypothetical release" occurred during 1 Feb – 1 Mar, 2001, 00 UTC at the Chernobyl NPP after a) 6 hours, b) 12 hours, c) 18 hours, and d) 24 hours.

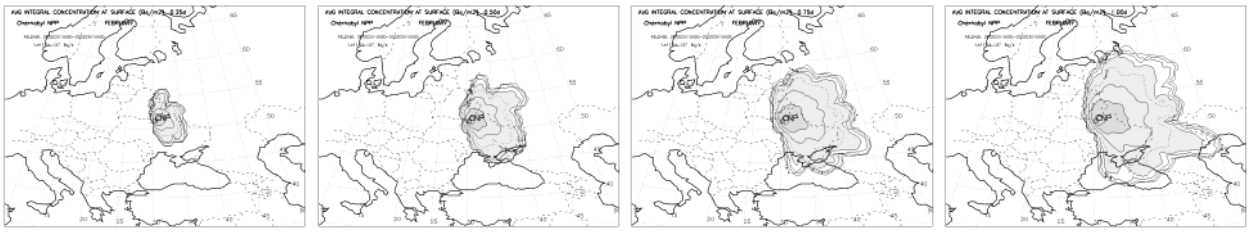

(a) (b) (c) (d)

Figure 4.1.5. Cs^{137} averaged integral concentration at surface fields as a result of the "unit hypothetical release" occurred during 1 Feb – 1 Mar, 2001, 00 UTC at the Chernobyl NPP after a) 6 hours, b) 12 hours, c) 18 hours, and d) 24 hours.

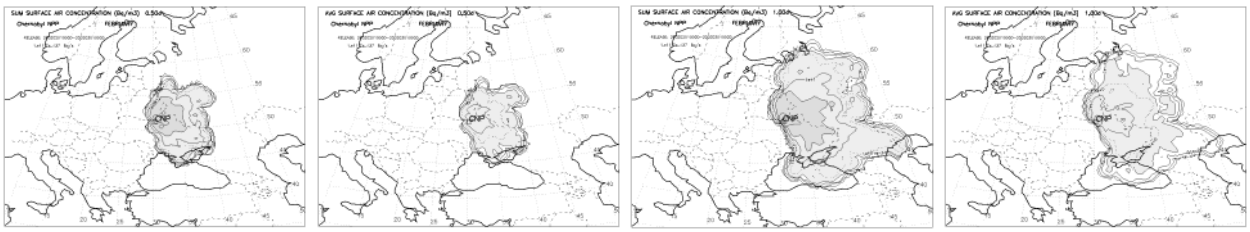

(a) (b) (c) (d)

Figure 4.1.6. Cs^{137} summary (a&b) and averaged (c&d) surface air concentration fields as a result of the "unit hypothetical release" occurred during 1 Feb – 1 Mar, 2001, 00 UTC at the Chernobyl NPP after 12 hours (a&c) and 24 hours (b&d).

Using a similar technique as it was realised for the airflow pattern and fast transport (*Baklanov and Mahura, 2001*), the wet and dry deposition, concentration and integral concentration fields (sum for the time period – month, and average - sum/#days in month) for the first hours, half-day or first day release transport can be constructed. Figures 4.1.4 – 4.1.6 give several examples of such kind of the dispersional indicators for the first 6, 12, 18, 24 hours separately and as integral as well as for particular threshold values for 5d trajectories.

4.2. *APPROACHES TO ANALYSIS OF DOSES*

Following the suggested methodology, as next step, for analysis of the risk levels and possible consequences for the population, an evaluation of the vulnerability to radioactive deposition, simulated in the previous chapters, concerning its persistence in the ecosystems; in particular, with a focus on the transfer of certain radionuclides into food-chains of key importance for the intake and exposure in the whole population and native groups of the Euro-Arctic regions (e.g. Saami) will be carried out.

For these purposes, we will use different dose calculation models (e.g. *MACCS, 1990; Balonov, 1999; Golikov, 2001; Wright et al., 2002*) and empirical correlations between fallout and human doses, which have been obtained on a basis of investigations of the nuclear tests and the Chernobyl accident effects on the Nordic countries (*Moberg, 1991; Selnæs and Strand, 1992; Dahlgaard, 1994; Brynildsen et al., 1996; Nielsen, 1998; Bergman and Ågren, 1999; ÖCB, 2000*). An analysis of the risk levels (potential contamination and exposure) and possible consequences for the population in the local/meso-scale will be carried out using models adapted for specific northern nutrition pathways. Some long-term consequences will be estimated also in the regional-scale using empirical models and correlation between fallout and doses for humans. This item is not discussed in details here, because it will be a topic for one of the following project reports. The Norwegian Radiation Protection Authority (NRPA), Swedish Defence Research Authority (FOI), the RISØ National Laboratory, Denmark and the Institute of Radiation Hygiene, St. Petersburg, Russia will take part in this work.

Radiological sensitivity of the Northern ecosystems

The boreal and subarctic parts of Northern Europe exhibit relatively high sensitivity with regard to fallout of radiologically important long-lived nuclides, due to generally higher yearly as well as long-term concentrations in the vegetation per unit fallout than prevalent south of the boreal zones. Frequent, high use of terrestrial food products from these northern areas therefore will lead to cumulative doses with significant contributions also during a long time after the occurrence of the initial environmental contamination. These generally very large differences in transfer to man and long-term availability in food-chains in the boreal region in comparison to areas further south – at least as far as ^{90}Sr and ^{137}Cs are concerned – need to be considered in assessments relating radioactive deposition to resulting internal exposure and dose.

Table 4.2.1 indicates the quotient between concentrations of ^{137}Cs in certain food products (Bq/kg) and the average deposition (Bq/m^2) covering the range frequently observed in the northern boreal zone *(Bergman et al 1995).* Levels in milk and beef, respectively, are about a factor 0.1 and 0.5 of that in the fodder.

As a guide to preliminary predictions of the radiological significance concerning the use of certain contaminated food items, ratios analogous to the factor **R** in the table appear helpful. The long-time intake of radioactive nuclides via food may be described as dependent on the amount

deposited; the activity concentration in the food product in comparison to that in the fallout; and the quantity consumed.

The sub-alpine and boreal pathways over fresh-water fish, reindeer, and moose, however, exhibit a persistent high long-term transfer in comparison to the products from the agricultural landscapes. The uptake in reindeer is particularly effective. Under the condition of equal deposition of ^{137}Cs over agricultural and forest landscapes, reindeer will contain activity concentration one to two order of magnitude higher than present in the agricultural products.

Long-term series of the ^{90}Sr and ^{137}Cs levels in milk from sub-alpine and north-boreal areas (*Suomela and Melin 1992*) also reveal a persistent availability.

Table 4.2.1: The ratio **R** [$Bq \cdot kg^{-1} / Bq \cdot m^{-2}$] between the activity concentration of ^{137}Cs in the food products and the ^{137}Cs deposition per m². Approximate levels after deposition over respectively Boreal forests and agricultural ecosystems are assessed for the first five years and at about a decade later,

Food component	**R** [m²/kg] ⊗	**R** [m²/kg] ⊗
Products from Boreal forests		
	The first five years	**A decade later**#
moose	0.01-0.02*	0.01- 0.02
reindeer	0.2-2**	0.01-0.5
fresh-water fish	0.1-0.5***	0.01-0.1
lingon- and bilberry	0.03-0.04*	0.01 -0.02
cloudberry	0.1*	0.02 - 0.05
mushrooms	0.1-1.5+	0.05 -1
Products from agricultural landscapes##		
Cereals, the seed	0.0002- 0.002	0.0002- 0.002
Potatoes	0.002 -0.02	0.002 - 0.02
Grass, arable land	0.002- 0.02	0.002 - 0.02
Grass, natural pasture	0.005 - 0.05	0.003 - 0.03

⊗ Dry matter weight for vegetables, fresh weight for animals.
* *Bergman et al,.1995*.
** Maximum levels in spring, minimum in end of summer.
*** Maximum levels obtained after 1-3 years in perch, trout and grayling; later in pike *Johansson et al., 1991*) .
\+ *Johansson and Bergström, 1994*.
\# Semi-qualitative assessment of long-term behaviour.
Based on uptake from the root-zone in areas with low and high content of clay.

Cumulative intake by man over food-chains of key importance

Under the assumption of an essentially unchanging consumption pattern over long time periods, the cumulative intake of each specific radionuclide by man depends on its persistence in the relevant ecosystems, and the effectiveness of transfer in the food-chains. Based on data as exemplified in table 4.2.1 forecasts of doses may be done for different time periods to assess the radiological consequences and need for countermeasures. To illustrate semi-qualitatively long-term trends in the intake, a comparison is made in Figure 4.2.1 (with physical decay taken into account)

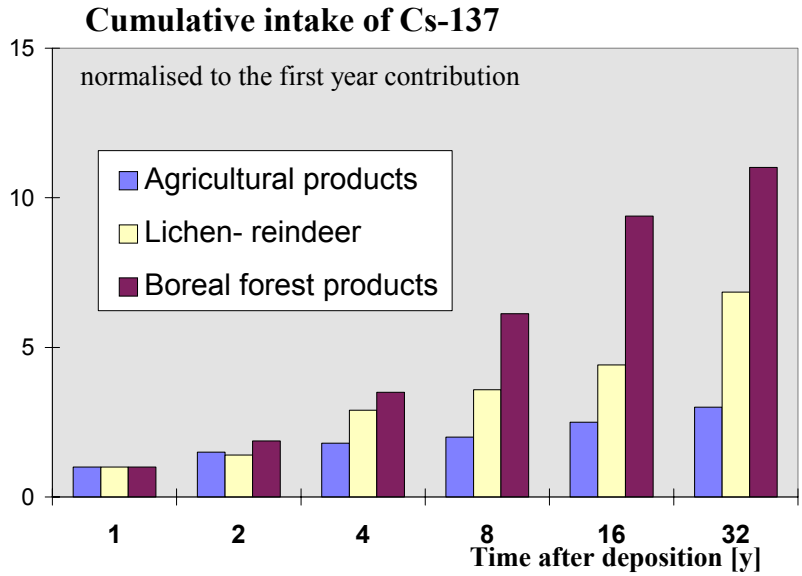

Figure 4.2.1. Cumulative intake of ^{137}Cs by food-products originating from a) agriculture (meat, milk and milk products) and b) reindeer meat, and c) boreal forest (game and berries) landscapes. The levels are normalised to the respective first year contribution.

normalised to the first year contribution from certain food-products of different origins: a) agricultural products, b) reindeer meat and c) boreal forest products. When normalised to the first year consumption, the sum of the contributions from each subsequent year to the cumulative intake reflects the time dependent efficiency in transfer for each of the three food products. As illustrated for ^{137}Cs in figure 1, transfer during long time is much more effective for the boreal forest food chains (e.g. berries and moose) and for the transfer via lichen-reindeer in comparison to that for the agricultural products: milk, milk products and meat. This means that in case of an unchanging consumption pattern during long time the fraction of the total cumulative intake contributed by the boreal forest food chains (including that over reindeer) will increase with time. In Sweden the ^{137}Cs intake by the general population from consumption of boreal forest products amounted to about 10% of the total intake during the first year after the Chernobyl accident (*Holmberg et al. 1988*). This means that the cumulative intake, as indicated by figure 1, should lead to contributions of similar size from boreal forest and agricultural products two to three decades after the radioactive deposition. For populations consuming forest products or reindeer meat to a higher extent than the population in general the intake from boreal forest food-chains are correspondingly more important.

4.3. *APPROACHES TO GIS BASED RISK ANALYSIS*

GIS-based analysis integrated with mathematical modelling gives a possibility to develop a common methodological approach for complex assessment of regional vulnerability and risk gathering separate aspects of study (modelling of consequences, probabilistic analysis of pathways, dose estimation, etc.). Furthermore, combined with the available geographic, demographic, administrative and economical databases, GIS-analysis allows evaluating the social and economical consequences for different geographical areas and population groups, especially native people in the Nordic countries (*Rigina, 2001; Rigina & Baklanov, 2002*).

There we tested two separate approaches to assess residential risk or territorial vulnerability to radiation risk from an NPP (Figure 4.3.1): probabilistic and deterministic (case-studies).

In the deterministic case we estimated the mean individual and collective doses for different groups of population, based on predicted concentration/deposition fields for a number of certain scenarios (most probable or worst cases) and the empirical correlations between the fallout and human doses (see Ch. 4.2).

In the probabilistic case, vulnerability was defined either as a product of scaled factors and probabilities or as product of probabilities and weighted sum of factors:

1) social-geophysical factors (proximity to NRSs, population density; critical groups of population; ecological vulnerability of area; risk perception, preparedness of safety measures and quick response systems; counteracting economical and technical consequences of accident) and

2) probabilities (accident of certain severity; atmospheric transport from NRSs; removal over area during atmospheric transport (the last two based on the atmospheric trajectory modelling)).

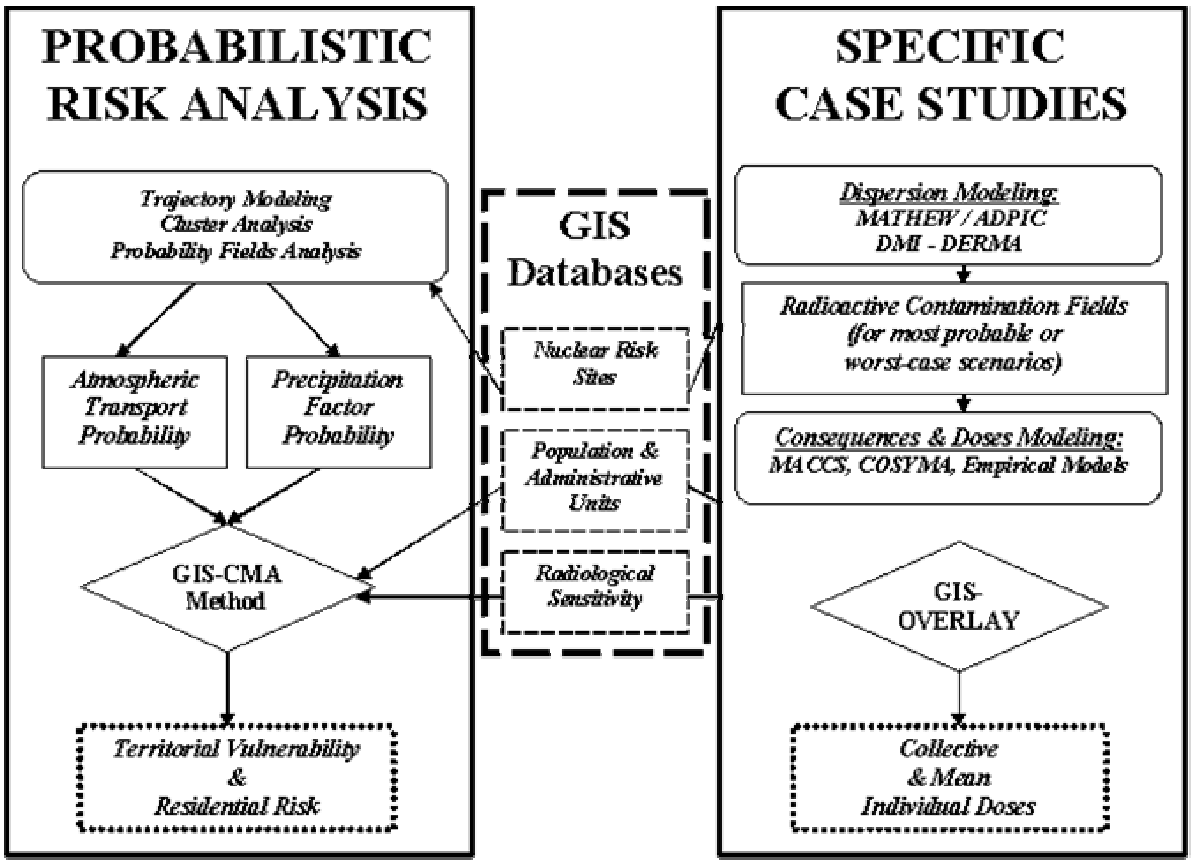

Figure 4.3.1. Scheme of the complex risk assessment based on the GIS integration and modelling.

In the deterministic case, the common GIS overlay method was applied, whereas in the probabilistic case, a more complex CMA method was necessary.

The current approach considering the long-term dispersion modelling is a logical continuation of the above-mentioned methods (*Rigina, 2001; Rigina, Baklanov, 2002*) and is a complementary

combination of both. In contrast to the previous approach, where we didn't have probabilistic fields of deposition, now annual/seasonal/monthly probabilistic concentration and deposition fields have been calculated based on the discussed in this report approach.

Some of the probabilities used in the earlier studies, such as atmospheric transport and precipitation factor during overpass, are accounted here implicitly, and thus, are excluded from calculation of vulnerability. All the factors and probabilities, not accounted implicitly, remain in the formula of risk/vulnerability. Also, mean individual and collective doses for different groups are now calculated from the concentration and deposition analogously to the specific case studies, but more accurately using dose calculation models (see Ch. 4.3) instead of empirical coefficients.

This approach allows avoiding many uncertainties in estimating the risk and vulnerability.

We don't go deeply in details because next report will be specially devoted to these issues.

V. METHODOLOGY FOR SPECIFIC CASE STUDIES

The suggested methodology for the complex risk and vulnerability assessments includes a combination of the probabilistic analysis of trajectory and long-term dispersion modelling, and the separate case studies (Figure 4.3.1). The efforts of this chapter focus on case studies of potential radionuclide releases including source terms and impacts on population of various geographic areas of the Euro-Arctic region.

Specific case study simulations, in comparison with the above-considered long-term dispersion modelling, have the following peculiarities: (i) higher space resolution and smaller time step for meteorological fields dynamics; (ii) many nuclides of the concern; (iii) different release heights; (iv) different continuation of releases; (v) more complex release composition (particle size etc.); (vi) different scenarios (time evolution of the release strength, etc.). Therefore the specific case studies give additional, very important information about the possible consequences in case of accidents for extreme or typical situations, which are not available from the probabilistic analysis.

We should note that this approach is computationally less expensive compared to dispersion modelling for a multiyear period, although it provides less reliable output and allows us to consider further risk and vulnerability analysis only on particular dates. Alternatively, this approach provides possibility of seeing potential consequences of an accident for worst-case meteorological situations. In this study, we followed several ways suggested by *Baklanov et al., 1994; INTAS, 2000; OCB, 2000* (for local scale) and *Bergman et al., 1998; Baklanov et al., 2001; Baklanov et al., 2002a,b; Mahura et al., 2002a* (for regional scale) on examples of the Kola NPP as well as nuclear submarines and spent nuclear fuel facilities in the northern latitudes.

For simulation of possible consequences on a regional scale, the DERMA model (*Sørensen, 1998; Sørensen et al., 1998; Baklanov and Sørensen, 2001*) with the DMI-HIRLAM (*Sass et al., 2000*) high-resolution meteorological data (E-version: 0.15° or G-version: 0.45°) will be used. DMI's 3D Lagrangian transport model calculates forward and backward trajectories for any point in the area.

5.1. *CRITERIA FOR SELECTION OF SPECIFIC CASE STUDIES*

As we discussed above for the complex risk assessments a combination of the both methods - a) the probabilistic risk assessment and b) the case study (Figure 4.3.1) - gives the most sufficient approach. Therefore, it is important to choose correctly the most representative episodes for typical and worst case scenarios.

The selection of specific cases with typical or worst-case scenarios can be based on results from trajectory modelling and probability field analysis. In general, several criteria could be used for specific case selection. First, the main direction of atmospheric transport of radioactive cloud of an accidental release at NRS should be toward the region of interest. In our study, these regions are the Nordic countries (Denmark, Finland, Iceland, Norway, Sweden, the Faeroe Islands) and the populated territories of the Russian North-West. Second, the possibility of precipitation during atmospheric transport of the radioactive cloud over the region of interest should be taken into account. In the suggested here methodology it could be inferred from the dispersion modelling of wet deposition patterns. Third, the relatively short travel time of the radionuclide cloud from the NRS location toward the region of interest (consideration of which depends on the fast transport probability field patterns) will be important. Forth, the relatively large coverage of the regions of interest by the radioactive cloud during atmospheric transport should be considered. And finally,

preferably, although not crucial, for the regional scale analysis, the stable boundary layer conditions and atmospheric transport is limited by the boundary layer height as well as for cold and warm seasons.

For the specific case studies, it is important also to consider common parameters of accidental radionuclide releases. Among these factors are the following: 1) duration of accidental release at selected location, 2) altitudes of initial plume rise, 3) distribution of particle sizes for considered radionuclides, and 4) reference deposition velocities. In this study, we selected three radionuclides - ^{137}Cs, ^{131}I, and ^{90}Sr – as major dose-contributing radionuclides. Additionally, for long-term releases/emissions (e.g., for the Sellafield reprocessing plant) we consider ^{129}I and ^{99}Tc. The major characteristics for each radionuclide used in dispersion modelling are shown in Table 5.1.1. It should be noted that for ^{131}I we used an average of the gaseous and particulate forms. During these specific dates, the releases at NRSs are the continuous "unit hypothetical releases" of radioactivity ($1 \cdot 10^{10}$ Bq/s) with the discrete emitting of puffs (every 60 minutes) during 24 hours, and a simulation of release in the boundary layer for the following 5 days of atmospheric transport after the occurrence of the accidental release.

Our detailed analysis for the NRS worst-case scenarios will be shown in next project report.

Table 5.1.1. Characteristics of radionuclides selected for dispersion modelling.

Radionuclide Characteristics	**^{137}Cs**	**^{131}I**	**^{90}Sr**	**^{129}I**	**^{99}Tc**
Half Life (s)	$9.50428 \cdot 10^{8}$	$6.94800 \cdot 10^{5}$	$9.17640 \cdot 10^{8}$	$4.95115 \cdot 10^{14}$	$6.62256 \cdot 10^{12}$
Reference Dry Deposition Velocity (m/s)	0.0015	0.006 (*	0.002	0.006	0.001 (**
Average Particle Radius (μm)	0.3	0.325	1.25	0.325	0.25

*) average value for all 3 forms (e/o/a) - (0.015/0.00015/0.0015), **) value by default.

5.2. *ANALYSIS FOR SPECIFIC CASE STUDIES*

Previously several case studies for the Kola nuclear power plant and nuclear submarine bases were also realised by *Baklanov* (2000) and *Baklanov et al*. (2002). *Bergman et al*. (1998), *Baklanov* (1999) and *Baklanov et al.* (2001) made several sensitivity studies of potential airborne radioactive contamination and consequences to different variations of the release parameters on examples of risk sources on the Kola Peninsula. These studies included the sensitivity to the type of nuclides, release heights, continuation of releases, release composition (e.g., particle size), deposition mechanisms etc.

Several specific case studies were considered for the 'Kursk' submarine lifting and decommissioning operations (*Mahura et al.,* 2002; *Baklanov et al*., 2002).

In this chapter, as an example of the specific case study, the potential risk of airborne contamination of the environment during the Kursk nuclear submarine (KNS) decommission operation in Snezhnogorsk (NW Russia) using the DERMA and DMI-HIRLAM models in forecasting mode is estimated. As a first approximation, the unit hypothetical release (UHR) (10^{11} Bq/s of ^{137}Cs) which occurred during up to 6 hours at the KNS location was considered. For the specific cases the simulation of the radionuclide surface air concentration (Bq/m^3), wet and dry deposition (Bq/m^2) fields was performed.

Let us consider the potential risk of airborne contamination for UHR of ^{137}Cs during the KNS operation phases, which include the removal of six damaged missiles and nuclear fuel from KNS in the "Nerpa" dry dock in Snejznogorsk (Murmansk region) during July-October 2002.

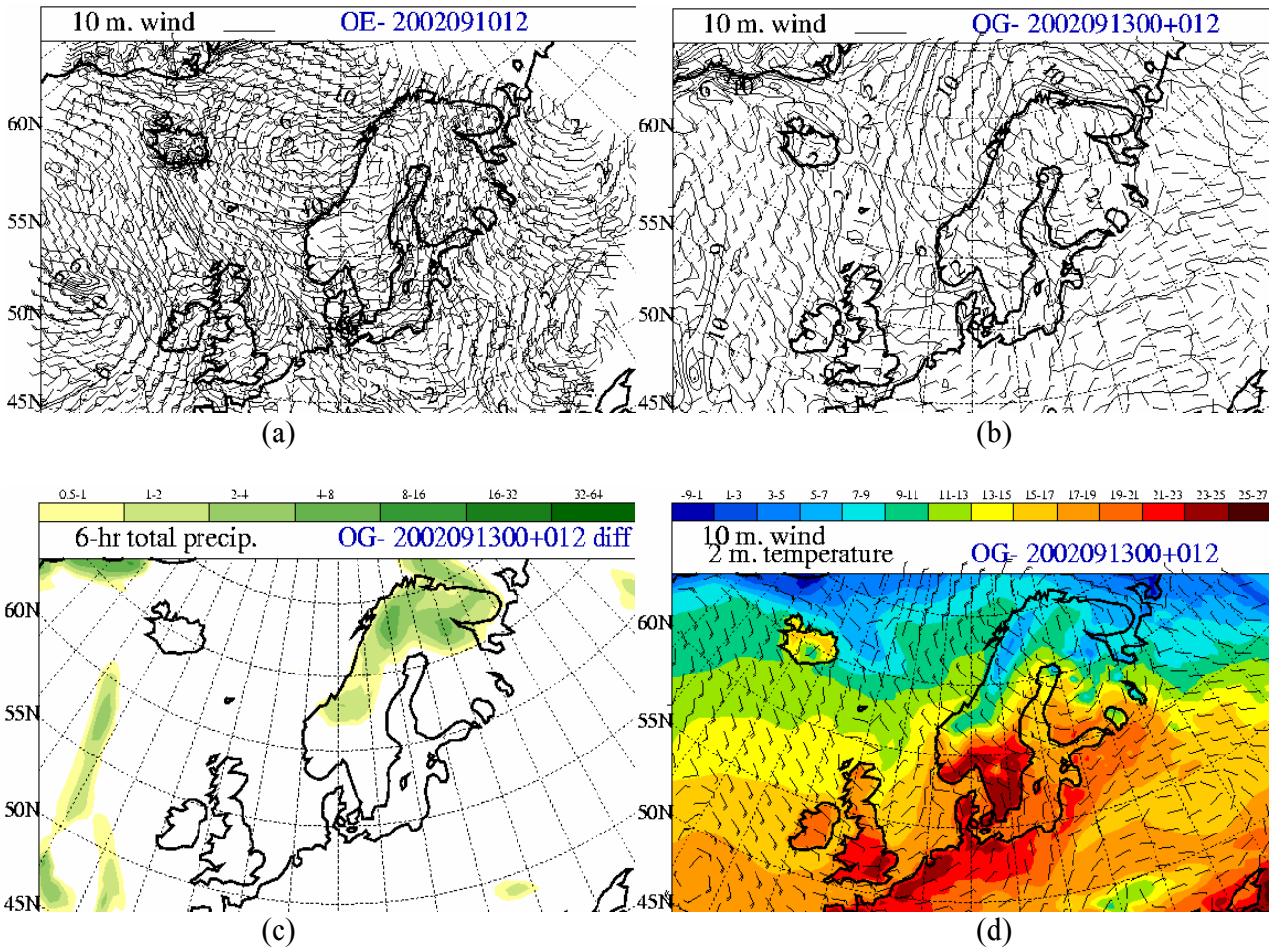

Figure 5.2.1. Specific case of 10 September 2002 - meteorological fields: a) analysed wind at 10 m for 10 Sep 2002, 12 UTC (DMI-HIRLAM, E-version), b) forecasted wind at 10 m for 13 Sep 2002, 12 UTC (DMI-HIRLAM, G-version), c) forecasted 6-hour precipitation for 13 Sep 2002, 12 UTC, and d) forecasted wind at 10 m and temperature at 2 m for 13 Sep 2002, 12 UTC.

The hypothetical release from the site started on 10 September 2002, 12 UTC, and it continued during 1 hour with the heights of the primary radioactive plume between 0-500 m. The remaining model input data and conditions are similar to the previous case studies.

The Figure 5.2.1 presents dynamics of the weather situation based on the DMI-HIRLAM numerical weather forecast for the region of interest during 10-13 September 2002. The wind field maps shown in Figure 5.2.1 represent the forecast by the E-version (15x15 km horizontal resolution) and G-version (45x45 km horizontal resolution) of the DMI-HIRLAM model. As shown in Figure 5.2.1a, the higher resolution version of the model has a limitation of the modelling domain close to the KNS location, and hence, depending on the wind direction from the site the E- or G-version for the dispersion modelling could be used.

The Figure 5.2.2 shows the calculated air concentration (Bq/m^3) in the mixing layer at different times after the beginning of UHR of ^{137}Cs from the risk site. The integrated in time surface air concentration ($Bq \cdot h/m^3$) and ground-contamination (total deposition as the sum of dry and wet depositions, in Bq/m^2) four days after the release start are shown in Figure 5.2.3.

During the first day, the radioactive plume is transported slowly over the Kola Peninsula and Karelia to the south, due to low wind velocity within the boundary layer for this meteorological situation. On the second day, the plume is also extended to the north over the Barents Sea. An intensive precipitation in the first days after the release gives a large area of maximal deposition of radionuclides over the Kola Peninsula and surrounding areas. On the third day, the plume continued to move in the south-east and east direction from the site, but concentration decreased quickly and considerably.

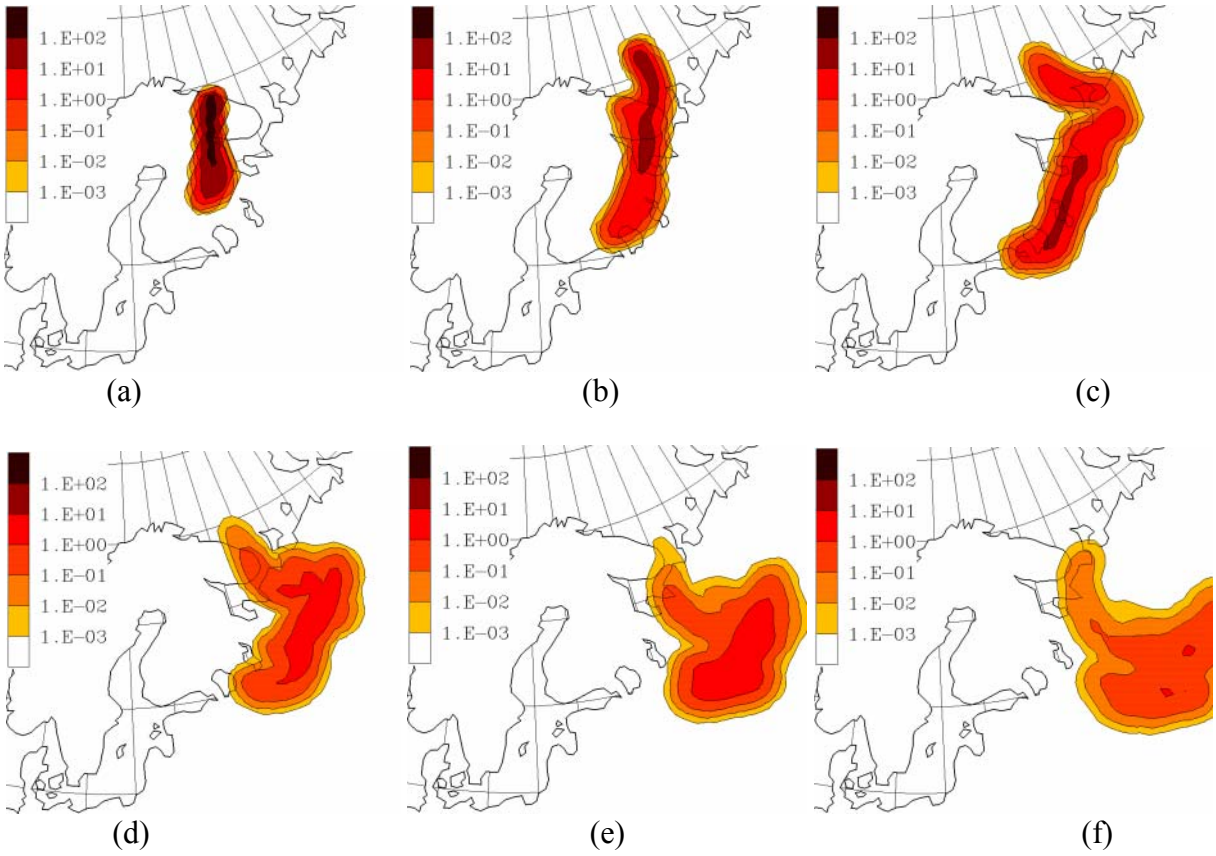

Figure 5.2.2. Specific case of 10 September 2002 for UHR of ^{137}Cs at the Snezhnogorsk shipyard (Nerpa): surface air concentration fields at: a) 11 Sep 2002, 00 UTC, b) 11 Sep 2002, 12 UTC, c) 12 Sep 2002, 00 UTC, d) 12 Sep 2002, 12 UTC, e) 13 Sep 2002, 00 UTC, and f) 13 Sep 2002, 12 UTC.

Evaluation of Possible Consequences

As it was mentioned above, the simulations were done for a discrete unit hypothetical release of ^{137}Cs. However, experts can easily recalculate the concentration and deposition fields for any particular release value.

Although the ship reactor accidents may lead to serious environmental consequences, some studies (*e.g. NACC, 1998*) indicate that any potential naval reactor accident will not be nearly as severe as the Chernobyl accident. Some calculations of airborne transport, deposition, and exposure have been made based on an assumed release of 1 PBq of ^{137}Cs (*NACC, 1998; Bergman et al., 1998*). It is not obvious that this amount would actually be released in an accident, even if it is available in the core. Moreover, the relative uncertainty of the release is estimated to be a factor of ten. The maximum content of ^{137}Cs in the first and second generation of the Russian ship reactors is

estimated to 5 PBq (*Gussgard, 1995*), while 10 PBq may be accumulated during operation of a typical modern ship reactor (i.e. with a power level slightly less than 200 MW). The KNS core inventory was not available in this study. However, a rough guess of the Bellona experts based on the known inventories of other submarines (*Gerdes et al., 2001; Bellona, 2001*) gives 6.2 PBq of ^{137}Cs and 5.6 PBq of ^{90}Sr.

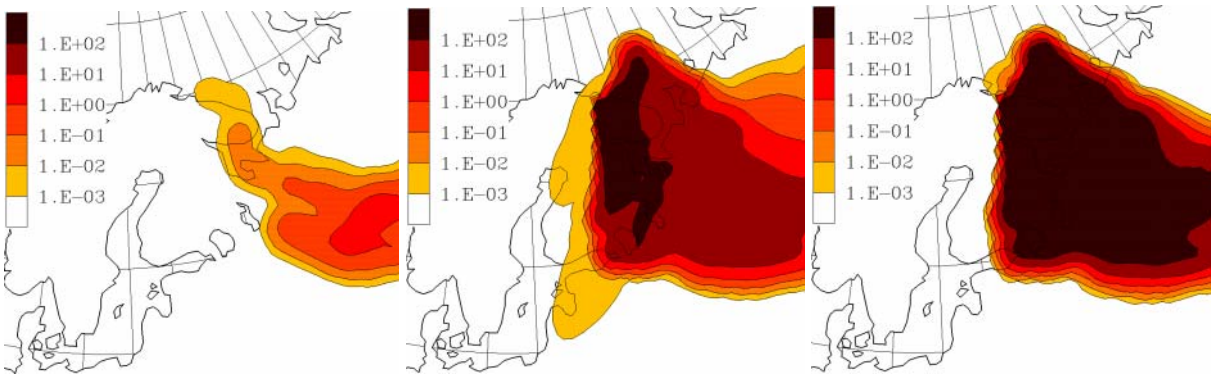

Figure 5.2.3. Specific case of 10 September 2002 for UHR of ^{137}Cs at the Snezhnogorsk shipyard: a) surface air concentration field at 14 Sep 2002, 00 UTC; b) integrated in time air concentration in the surface layer field at 15 Sep 2002, 18 UTC, and c) total deposition field at 14 Sep 2002, 00 UTC.

Our calculation (based on Figure 5.2.3) for the total unit release (1Bq) case indicates that the large areas of the Northwest Russia (excluding the Kola Peninsula) could obtain deposition of a fraction of the order of 10^{-13} Bq/m^2. This corresponds to a deposition of 100 Bq/m^2 per 1 PBq of airborne release of ^{137}Cs in the accident, i.e. the level used in the *NACC (1998)* study. On the Kola Peninsula the higher deposition density (one to two orders of magnitude) might be expected compared with the Northwest Russia. In our case, 1 PBq of ^{137}Cs airborne release corresponds to 1-10 kBq/m^2 and up to 50 kBq/m^2 on the Kola Peninsula vs. local scale close to the release site.

For Scandinavia, the direct deposition of ^{131}I or ^{137}Cs on pasture and crops at levels falling below 1 kBq/m^2 is not likely leading to restrictions in normal agricultural practice or formal acceptance for commercial use of the food-products (*Bergman et al., 1998*). The concentration in reindeer in the Northern Fennoscandia is high, when feeding during winter on lichens exposed to fallout of radioactive caesium (^{134}Cs and ^{137}Cs). The ratio between activity concentration in the reindeer meat and deposition density will be close to 1 kg/m^2 in the latter half of the first winter season after the fallout (*Bergman & Ågren, 1999*). This implies contamination about one order of magnitude higher than concerning direct deposition in the sensitive food-chain of grass-cow-milk. Intake of radioactive caesium in population groups consuming much reindeer meat is expected to be high.

Assuming a release of 1 PBq of ^{137}Cs and following *Bergman et al., 1998*, the levels of this radionuclide attained in reindeer meat are expected to be: 1) 1 kBq/kg in large areas on the Kola Peninsula affected by deposition, and 2) one order of magnitude higher over some small areas within a hundred kilometres from the site of release.

It should be stressed that we do not link the hypothetical accident releases considered in the above analysis with the “Kursk” submarine case. In our analysis, we simply discussed possible consequences and their scales after the most severe hypothetical accident with a ship nuclear reactor. Moreover, it should be noted that all completed high and medium potential risk level

phases/actions of the KNS operation were performed successfully, and none of them involved any radioactive contamination or real risk for the population and the environment.

CONCLUSIONS AND RECOMMENDATIONS

In this study, we have developed a methodology for complex risk and vulnerability assessment and mapping. The main question to answer was: Which regions are at the highest risk from a hypothetical accidental release at an NRS in the study region?

To answer this question we suggest applying a variety of research tools considering them as a sequence of interrelated approaches. Among these tools are the following: atmospheric trajectory and dispersion modelling, methods of statistical analysis, specific case studies, evaluation of vulnerability to radioactive contamination, and risk evaluation and mapping.

In comparison with the previous studies the methodology considered in this report focuses on the long-term dispersion and deposition modelling, statistical analysis of dispersion modelling results as well as briefly outlines the methods for the dose calculation and assessment of regional vulnerability and residential radiation risk, based on GIS modelling and analysis.

We assume that the suggested approach for complex risk assessment provides useful information for further studies. Such results are applicable for the:

(i) initial estimates of the probability of atmospheric transport and deposition in case of an accidental release at an NRS;
(ii) improvement of emergency preparedness to possible accidents at an NRS;
(iii) social and economical consequence studies of the impact for the populations and environment of the neighbouring countries;
(iv) multidisciplinary risk and vulnerability analysis, probabilistic assessment of radionuclide meso-, regional-, and long-range transport; as well as
(v) modelling and testing of higher-resolution models.

ACKNOWLEDGMENTS

The authors are grateful to Leif Laursen (Danish Meteorological Institute, Denmark), Boris Segerståhl (Thule Institute of University of Oulu, Finland), Sven Nielsen (Risø National Laboratory, Denmark), and Steen C. Hoe (Danish Emergency Management Agency, Denmark) for collaboration, discussions and constructive comments.

The computer facilities at the Danish Meteorological Institute (DMI) have been used extensively in the study. The DMI-HIRLAM and ECMWF meteorological data were used as input data for the dispersion modelling. The authors are grateful to the HIRLAM group and to the Data Processing Department at DMI for the collaboration, computer assistance, and advice.

Financial support of this study included the grants of the Nordic Arctic Research Programme (NARP) and Nordisk Forskerutdanningsakademi (NorFA).

REFERENCES

Amosov, P.V., A.A. Baklanov and S.I. Mazukhina (1995) Estimation of potential risk for the population from the hypothetical accident at the Kola nuclear power plant. In: *The 2nd International Conference on Environmental radioactivity in the Arctic*. Oslo, August 21-25, 1995, pp. 365-368.

Andreev, I., Gazso, A., Gohla, H., Hofer, P., Kromp, W., Kromp-Kolb, H., Rehm, W., Seibert, P. (2000) Risks due to severe accidents of nuclear power plants in Europe - the methodology of RISKMAP – Possible extensions. In: *ESEE 2000: 3rd Int. Conference of the European Society for Ecological Economics*.

Andreev, I., Hittenberger, M., Hofer, P., Kromp-Kolb, H., Kromp, W., Seibert, P., Wotawa, G. (1998) Risks due to severe accidents of nuclear power plants in Europe - the methodology of riskmap. *J. Hazardous Materials*, **61**, 257-262.

ANWAP (1997) *Radionuclides in the Arctic seas from the former Soviet Union: Potential health and ecological risks*. Eds. D. Layton, R. Edson and B. Napier. Arctic Nuclear Waste Assessment Program, Office of Naval Research (ONR), USA.

AR-NARP (2001-2003) On-going Project ´Atmospheric Transport Pathways, Vulnerability and Possible Accidental Consequences from the Nuclear Risk Sites in the European Arctic (*Arctic Risk*`)` of the NARP: Nordic Arctic Research Programme. *DMI* project web site: http://www.dmi.dk/f+u/luft/eng/arctic-risk/main.html).

Baklanov, A. (1995) Radiation risk objects at the Northern-West Russia and estimation of radiation consequences after hypothetical accidents. In: *Probabilistic Safety Assessment Methodology and Applications (PSA'95),* Proceedings of the International Conference. Volume 1. Seoul, Korea, Korea Atomic Energy Research Institute, pp. 532-536.

Baklanov, A. (1999) Parameterisation of the deposition processes and radioactive decay: A review and some preliminary results by the DERMA model. *DMI Scientific Report*, No. 99-4. 40 pp.

Baklanov, A. (2000) Modelling of episodes of atmospheric transport and deposition: Hypothetical nuclear accidents in North-West Russia. In: *Nuclear Risks, Environmental and Development Cooperation in the North of Europe*. CERUM, University of Umea, Sweden, pp. 57-72.

Baklanov, A. (2002) Methodologies for multidisciplinary nuclear risk and vulnerability assessments in the Arctic and Sub-Arctic. *NATO Science Series, Kluwer Academic Publishers*, (in press)

Baklanov, A. & R. Bergman (1998) Radioactive sources in the Kola-Barents region: Which ones may constitute a hazard now or for the future?, In: *Civil beredskap: Risk, kris, säkerhet och sårbarhet i samhället*. C. Löfstrand, editor. ÖCB and Umeå Universitet, Sweden, pp.31-41.

Baklanov, A. & Bergman, R. (1999) Radioactive Sources in the Barents Euro-Arctic Region: Are there reasons to be concerned?, Chapter XI at the *NEBI Yearbook: North European and Baltic Sea Integration*, Copenhagen, Springer-Verlag, pp. 171-192.

Baklanov, A., R. Bergman, B. Segerståhl & L. Thaning (1996) Assessment of risk of airborne radioactive contamination from nuclear units in north-west Russia. In: *2000 then what? Proceedings of the 13th International Clean Air and Environment Conference*. Adelaide, Australia, 22-25 September 1996/ Edited by A. Smith. CASANZ, Australia, pp.127-133.

Baklanov A., R. Bergman, C. Lundström and L. Thaning (2001) *Modelling of episodes of atmospheric transport and deposition from hypothetical nuclear accidents on the Kola peninsula*. CERUM Northern Studies No. 23. Umeå university, Sweden.

Baklanov A., Mahura A. (2001) *Atmospheric Transport Pathways, Vulnerability and Possible Accidental Consequences from the Nuclear Risk Sites: Methodology for Probabilistic Atmospheric Studies*. DMI Sci. Report #01-09. ISBN: 87-7478-450-1, 43 p., http://dmi.dk/f+u/publikation/vidrap/2001/Sr01-09.pdf

Baklanov, A.A., A.G. Mahura and S.V. Morozov (1994) The Simulation of Radioactive Pollution of the Environment After an Hypothetical Accident at the Kola Nuclear Power Plant**.** *J. Environmental Radioactivity,* **25**, 65-84.

Baklanov, A., A. Mahura, D. Jaffe, L. Thaning, R. Bergman, R. Andres, J. Merrill (1998) Atmospheric Transport Pathways and Possible Consequences after a Nuclear Accident in North-West Russia. *The 11th World Clear Air and Environment Congress*. S. Africa, Durban. 14-18 September 1998. Volume 2. E6-1: 6 pp.

Baklanov, A., A. Mahura, D. Jaffe, L. Thaning, R.Bergman, R.Andres (2002a) Atmospheric Transport Patterns and Possible Consequences for the European North after a Nuclear Accident. *Journal of Environmental Radioactivity,* **60**, 23-48.

Baklanov A., Mahura A., Rigina O. (2002b) Nuclear Risk and Vulnerability: Approach for Multidisciplinary Assessments. *Proceedings of the International Conference on Radioactivity in the Environment*, Principality of Monaco, 2-5 September 2002, Ed. P. Børretzen, T. Jølle, P. Strand, IUR-NRPA-JER-IAEA publ., pp. 87-92.

Baklanov, A., A. Mahura and J.H. Sørensen (2002c) Methodology for Prediction and Estimation of Consequences of Possible Atmospheric Releases of Hazardous Matter: 'Kursk' Submarine Study. Submitted to *Atmospheric Chemistry and Physics*.

Baklanov, A., O. Rigina, A. Mahura (2002d) Nuclear Risk and Vulnerability in the Arctic: New Method for Multidisciplinary Assessments. In: The 5th International conference on *Environmental Radioactivity in the Arctic*, St-Petersburg, Russia, June 16-20, 2002. NRPA, Oslo; pp 397-400.

Baklanov A., Sørensen J.H., (2001) Parameterisation of radionuclide deposition in atmospheric dispersion models. *Phys. Chem. Earth, (B)*, **26**, 787–799.

Baklanov, A.A., N.L. Tausnev, S.V. Morozov, L.S. Nazarenko, A.A. Zolotkov, L.M. Bakulin, I.V. Barsukov, O.Yu. Rigina, I.A. Rodyushkina, A.V. Smagin, E.M. Klyuchnikova, S.Dg. Cherepanov, A.G. Mahura and S.Yu. Limkina (1992) *Determination of risk zones and elaboration of scenarious of extreme radiologically dangerous situations in the Northern areas*. Report for the Russian Federation Ministry of Environment according to Project 'RISK' (#2416) of the State Programme 'Ecological Safety of Russia', Apatity: INEP KSC RAS, 179 p.

Bellona, 2001: http://www.bellona.no/

Bergman, R., editor (1999) *Assessment of potential risk of environmental radioactive contamination in northern Europe from terrestrial nuclear units in north-west Russia*. INTAS project 96-1802I. Technical report # 1 for February 1998- February 1999. May 1999, FOA-R—99-01080-861—SE, 109 p.

Bergman, R. & Baklanov, A. (1998) *Radioactive sources in main radiological concern in the Kola-Barents region*. FRN-FOA publication, Stockholm, July 1998. 82 p.

Bergman R, Larsson T, Andersson I, Edvarson K, Eriksson A, Finck R, Johansson K-J, Karlström F, Lönsjö H, Preuthun J, Ulvsand T och Wickman M. (1995) Radiakprobiern inom livsmedelssektorn: En studie inriktad på behoven för beslutsfattancle i tidigt skede efter radioaktivt nedfall. FOA-R--95-00140-4.3--SE.(in Swedish)

Bergman, R., Thaning, L. & Baklanov, A. (1998) *Site-sensitive hazards of potential airborne radioactive release from sources on the Kola Peninsula*. FOA report: FOA-R—00717-861--SE, February 1998, 14 pp.

Bergman, R. and Ulvsand, T. (1994). Intervention in regular practice to bring down external exposure to agricultural personnel or activity transfer over certain boreal food-chains. FOA report, National Defence Research Establishment, Dept of NBC Defence, S-90182 Umeå, Sweden.

Bergman, R. and G. Ågren (1999) Radioecological Characteristics of Boreal or Sub-Arctic Environments in Northern Sweden: focus on long-term transfer of radioactive deposition over food-chains. In: The 4th International conference on *Environmental Radioactivity in the Arctic*, Edinburgh, Scotland, Sept. 20-23, 1999, pp. 91-94.

Bergman, R. and Ågren, G. (2000) Radioecological Sensitivity of Certain Boreal or Sub-Arctic Environments and Implications for Dose Assessments. In: *Nuclear Risks, Environmental and Development Cooperation in the North of Europe*. CERUM, University of Umea, Sweden, pp. 97-103.

Bossew, P., M. Ichikawa, G. Mraz, G. Wallner and A. Wenisch (2000) Radiological investigations in the surroundings of Bilibino, Chukotka, Russia, *Journal of Environmental Radioactivity* **51**, 299-319

Brynildsen L, Selnæs T, Strand P & Hove K (1996) Countermeasures for radiocesium in animal products in Norway after the Chernobyl accident - Techniques, effectiveness and costs. *Health Physics* **70**(4), 1-8.

Crandall, W.K., C.R. Molenkamp, A.L. Wiliams, M.M. Fulk, R. Lange & J.B. Knox (1973) *An investigation of scavenging of radioactivity from nuclear debris clouds: research in Progress*. Lawrence Livermore National Laboratory, California, USA, Report UCRL-51328.

Dahlgaard, H., Editor (1994) Nordic Radioecology: The transfer of radionuclides through Nordic ecosystems to man. Amsterdam, Elsevier Science B. V. *Studies in Environmental Science* **62**.

Fullwood, R. (1999) *Probabilistic Safety Assessment in the Chemical and Nuclear Industries*. Butterworth-Heinemann, ISBN: 0750672080.

Gerdes, R., M. Karcher, F. Kauker, C. Köberle, (2001): Predicting the spread of radioactive substances from the Kursk. *Eos, Transactions, American Geophysical Union*, 82(23): 253, 256-257.

Gifford, F.A. (1984) The random-force theory: Application to meso- and large-scale atmospheric diffusion. *Boundary-Layer Meteorology*, **30**: 159-175.

Golikov, V. Editor (2001) Operational models for calculation of internal and external doses in the Arctic. Deliverable for the EC project AVAIL"Arctic vulnerability to radioactive contamination", Contract number: ERB IC 15-CT98-020, *Report of the* Institute of Radiation Hygiene, St. Petersburg, Russia & Norwegian Radiation Protection Authority, Oslo, Norway.

Graziani, G., W. Klug & S. Moksa 1998: Real-Time Long-Range Dispersion Model Evaluation of the ETEX First Release. EU JRC.

Gussgard, K. (1995). Is spent nuclear fuel at the Kola Coast and dumped in waters a real danger? In: P. Strand and A. Cooke (eds.): Environmental Radioactivity in the Arctic, Østerås, pp. 400-404.

Hales, J.M. (1986) The mathematical characterisation of precipitation scavenging. In: *The Handbook of Environmental Chemistry* / O. Hutzinger, editor, Vol. 4, Part A, pp. 149- 217.

Hinds, W.C. (1982) *Aerosol Technology*. Wiley, New York. pp. 38-68 & 211-232.

Holmberg M, Edvarson K and Finck R. (1988) Radiation doses in Sweden resulting from the Chernobyl fallout: a review. *Int. J. Radiation Biology*. **54**: 151.

Hongisto, M. (1998) *HILATAR, A regional scale grid model for the transport of sulphur and nitrogen compounds. Description of the model. Simulation results for the year 1993*. Finnish Meteorological Institute, Helsinki, No 21.

Howard, B.J., S.M. Wright, C.L. Barnett, L. Skuterud and P. Strand (2002) Estimation of critical loads for radiocaesium in Fennoscandia and Northwest Russia*, Journal of Environmental Radioactivity* **60**, 209-220

IAEA (1992a) Probabilistic Safety Assessment – A Report by the International Nuclear Safety Advisory Group. IAEA Safety Series No. 75-INSAG-6.

IAEA (1992b) Procedures for Conducting Probabilistic Safety Assessment of Nuclear Power Plants (Level 1). IAEA Safety Series No. 50-P-4.

IAEA (1995) Procedures for Conducting Probabilistic Safety Assessment of Nuclear Power Plants (Level 2). IAEA Safety Series No. 50-P-8.

IAEA (1996) Procedures for Conducting Probabilistic Safety Assessment of Nuclear Power Plants (Level 3). IAEA Safety Series No. 50-P-12.

IIASA (1996) Baklanov A., Bergman R., Segerståhl B. *Radioactive sources in the Kola region: Actual and potential radiological consequences for man*. Report, International Institute for Applied Systems Analysis. Laxenburg, Austria, IIASA, Radiation Safety of the Biosphere, 255 p.

INTAS (2000) *Assessment of Potential Risk of Environmental Radioactive Contamination in Northern Europe from Terrestrial Nuclear Units in North-West Russia*. Final Research Report of the Kola team, INTAS Project 96-1802, November 2000, Apatity-Umeå. 125 p.

Jaffe, D, Mahura, A & Andres, R (1997a) *Atmospheric Transport Pathways to Alaska from Potential Radionuclide Sites in the Former Soviet Union*. Research Report, UAF-ADEC Joint Project 96-001, p 71.

Jaffe, D, Mahura, A, Andres, R, Baklanov, A, Thaning, L, Bergman, R and Morozov, S. (1997b) *Atmospheric Transport from the Kola Nuclear Power Plant*. Research Report, UAF-FOA-BECN Joint Project, BECN: Tromsø University, Norway, Fall 1997, 61 pp.

Johansson K-J and Bergström R. (1994) Radiocaesium transfer to man by products from the forest. *Sci. Total Environ*. **57**: 309-316.

Johansson L, Wickman G, Ågren G, Eriksson A, Jonsson H and Tavelin B. (1995) Distribution of radioactive caesium in the population of northern Sweden 1988-1993. *Rad. Prot. Dosim*., **62**.

Karlsson, E. & Nyholm, S. (1998) Dry deposition of toxic gases to and from snow surfaces. *Journal of Hazardous Materials*, **60**: 227-245.

Kromp, W., (2002) Institute of Risk Research, Vienna, Austria. Personal communications.

MACCS (1990) *MELCOR Accident Consequence Code System (MACCS): Model Description*. Sandia National Laboratory, USA.

Mahura A., (2001) Probabilistic Assessment of Atmospheric Transport Patterns from Nuclear Risk Sites, *Ph.D. Phys.&Math. Thesis*, Russian State Hydrometeorological University/ Kola Science Center, Russian Academy of Sciences, 172p. (in Russian)

Mahura A., Andres R., Jaffe D. (2001) *Atmospheric transport patterns from the Kola Nuclear Reactors.* CERUM Northern Studies No. 24. Umeå university, Sweden. 33 p.

Mahura A., Baklanov A., (2002a) Probabilistic Analysis of Atmospheric Transport Patterns from Nuclear Risk Sites in Euro-Arctic Region. *Danish Meteorological Institute, DMI Scientific Report*, Fal 2002, 87p.

Mahura A., Baklanov A., (2002b) Probabilistic Indicators of Atmospheric Transport for Emergency Preparedness. Submitted to *Environment International*, 8p.

Mahura, A., Baklanov, A. & Sørensen, J. H. (2002a) Methodology for evaluation of possible consequences of accidental atmospheric releases of hazardous matter. Accepted for *Journal of Radiation Protection Dosimetry.*

Mahura, A., Baklanov, A., Rigina, O., Parker F.L (2002b) Statistical Analysis of Atmospheric Transport from the Nuclear Risk Sites in the Arctic Region. In: The 5th International conference on *Environmental Radioactivity in the Arctic*, St-Petersburg, Russia, June 16-20, 2002, pp 119-123.

Mahura, A.G., Jaffe, D., Andres, R. & Merrill, J. (1999) Atmospheric transport pathways from the Bilibino nuclear power plant to Alaska. *Atmospheric Environment*, **33**/**30**, 5115-5122.

Marchuk G.I., Aloyan A.E., Arutyunyan V.O., Louzan P.I. (1999) *Modelling of the Regional and Global Transport of Radionuclides from the Kola NPP*. INTAS project Report FOA-R-99-01390-861--SE

Maryon R.H., D. B. Ryall, (1996) *Developments to the UK nuclear accident response model (NAME)*. Department of Environment, UK Met. Office. DoE Report # DOE/RAS/96.011.

Merrill, J., Bleck, R. and Boudra, D.B. (1986) Techniques of Lagrangian Trajectory Analysis in Isentropic Coordinates. *Monthly Weather Review,* **114**, 571-581.

Moberg, L., Editor (1991) *The Chernobyl fallout in Sweden. Results from a research programme on environmental radiology*. The Swedish Radiation Protection Institute, Stockholm, Sweden.

Müller, H. & G. Pröhl (1993) ECOSYS-87: A dynamic model for assessing radiological consequences of nuclear accidents. *Health Physics*, V.64, n. 3, 232-252 pp.

NACC (1998) *Cross-border environmental problems emanating from defence-related installations and activities*. Vol 1. Phase 1: 1993-1995. Report no 204. North Atlantic Treaty Organisation.

Nielsen, S.P. (1998) A sensitivity analysis of a radiological assessment model for Arctic waters. *Radiat. Prot. Dosim*., **75**, 213-218.

Näslund, E. and Holmström, H. (1993) *Inclusion of a three-dimensional washout coefficient in ADPIC.* Report UCRL - ID-114054, Lawrence Livermore National Laboratory, California, USA.

ÖCB (2000) *Nuclear Risks, Environmental and Development Cooperation in the North of Europe*. CERUM Northern Studies, University of Umeå, Sweden, ISBN 91-7191-789-6. 240 p.

OTA (1995) *Nuclear Wastes in the Arctic. An Analysis of Arctic and Other Regional Impacts from Soviet Nuclear Contamination*. Washington, Office of technology Assessment. Congress of the United States.

Penenko, V. and A. Baklanov (2001) Methods of sensitivity theory and inverse modelling for estimation of source term and nuclear risk/vulnerability areas. *Lecture Notes in Computer Science*, Springer, Berlin, V. **2**, 57-66 (available also as a DMI Scientific Report, No. 01-04, http://dmi.dk/f+u/publikation/vidrap/2001/Sr01-04.pdf)

Prahm, L.P. & R. Berkowicz (1978) Predicting concentration in plumes subject to dry deposition. *Nature*, 271, 232-234.

Radke, L.F., E.E. II Hindman & V.P. Hobbs. (1977) A case study of rain scavenging of aerosol particles from an industrial plume. Proc. Symp. On Precipitation Scavenging, 1974. *ERDA Symp. Series*. NTIS, pp. 425-436.

Rantalainen, L. (1995) Source terms of the Kola nuclear power plant and risk of severe environmental contamination. In: The 2nd International Conference on *Environmental radioactivity in the Arctic*. Oslo, August 21-25, 1995.

Rigina, O. (2001) *Integration of Remote Sensing, mathematical modelling and GIS for complex environmental impact assessment in the Kola Peninsula, Russian North,* PhD thesis (April 2001), Geographical Institute of Copenhagen University; Copenhagen, Denmark: IGUK press. ISSN 0908-6625; ISBN 87-87945-49-5

Rigina, O. & Baklanov, A. (1999) Integration of mathematical modelling and GIS-analysis for radiation risk assessment. Presentation at the International Conference *'Nuclear Risks, Environmental and Development Cooperation in The North of Europe'*, Apatity, Russia, June 19-23, 1999.

Rigina, O. & Baklanov, A. (2002) Regional radiation risk and vulnerability assessment by integration of mathematical modelling and GIS-analysis. *Environment International*, **27**, 527-540.

Saltbones J., A.Foss, J.Bartnicki (2000) Threat to Norway from potential accidents at the Kola nuclear power plant. Climatological trajectory analysis and episode studies. *Atmospheric Environment*, **34**(3), 407-41

Sass, B. H., Nielsen, N. W., Jørgensen, J.U., Amstrup, B. and Kmit, M. (2000) The operational HIRLAM system, *DMI Technical report* 00-26. Copenhagen, Denmark. http://www.dmi.dk/f+u/publikation/tekrap/2000/Tr00-26.pdf.

Segerståhl, B., Ed. (1991) *Chernobyl: A policy response study*. Springer Series on Environment Management. Berlin, Heideiberg, NewYork, Springer-Verlag.

Segerståhl, B., A. Baklanov, R. Bergman, A. Mahura, O. Rigina, S. Nielsen, J.H. Sørensen and L. Westin (2001) Atmospheric transport patterns and risk in the European North after a nuclear accident. In: *The 1st Nordic Arctic Research Programme Symposium "The Arctic on Thinner Ice", 10–11 May 2001, Oulu, Finland.*

Seinfeld, J.H. (1986) *Atmospheric chemistry and physics of air pollution*. A Wiley-Interscience Publication. New-York.

Selnæs, T.D., Strand, P. (1992) Comparison of the uptake of radiocaesium from soil to grass after nuclear weapons tests and the Chernobyl accident. *Analyst*, **117**.

Simmons, A.J. & Gibson, J.K., Eds. (2000) ERA-40 Project Report series. 1. The ERA-40 Project Plan. ECMWF, 62p.

Sinyak, Y. (1995) Nuclear Energy in Eastern Europe and the Former Soviet Union: How Safe and How Much?, International Institute for Applied Systems Analysis (IIASA), report.

Slaper, H., Eggink, G.J., Blaauboer, R.O. (1994) *Risk assessment method for accidental releases from nuclear power plants in Europe*. Report of the National Institute of public health and the environment. Bilthoven, Netherlands.

Smith, F.B. (1968) Conditioned particle motion in a homogeneous turbulent field. *Atmos. Environ*. **2**, 491-508.

Smith, F. (1998) Estimating the Statistics of Risk from a Hazardous Source at Long Range, *Atmospheric Environment*, **32**(16): 2775-2791.

Sørensen, J.H. (1997) Sensitivity of DERMA to boundary-layer parameters, and evidence for meso-scale influence on long-range transport. In: ETEX Symposium on Long-range Atmospheric Transport, Model Verification and Emergency Responds. Ed. K. Nodop, Vienna, Austria, 13-16 May 1997, EUR 17346 EN, pp. 207-210.

Sørensen, J.H. (1998) Sensitivity of the DERMA Long-Range Gaussian Dispersion Model to Meteorological Input and Diffusion Parameters. *Atmos. Environ*. **32**, 4195-4206.

Sørensen J.H., Laursen L., Rasmussen A. (1994) Use of DMI-HIRLAM for Operational Dispersion Calculations. *Air Pollution Modelling and Its Application* X, edited by S.-E.Gryning & M.M.Millan, Plenum Press, pp. 373-381.

Sørensen, J.H., A. Rasmussen (1995) Calculations performed by the Danish Meteorological Institute. In: Report of the Nordic Dispersion/Trajectory Model Comparison with the ETEX-1 Fullscale Experiment. Eds. Tveten, U. and Mikkelsen, T., Risø-R-847(EN), NKS EKO-4(95)1, pp. 16-27.

Sørensen, J.H., Rasmussen, A. and Svensmark, H. (1996) Forecast of Atmospheric Boundary-Layer Height for ETEX Real-time Dispersion Modelling, *Phys. Chem. Earth*, **21**, No. 5-6, 435-439.

Sørensen, J.H., A. Rasmussen, T. Ellermann and E. Lyck (1998) Mesoscale Influence on Long-range Transport; Evidence from ETEX Modelling and Observations, *Atmospheric Environment,* 32, 4207-4217.

Strand, P., B.J. Howard, A. Aarkrog, M. Balonov, Y. Tsaturov, J.M. Bewers, A. Salo, M. Sickel, R. Bergman, K. Rissanen (2002) Radioactive contamination in the Arctic sources, dose assessment and potential risks, *Journal of Environmental Radioactivity,* **60**, 5-21.

Suomela J and Melin J. (1992) Förekomsten av cesium och strontium-90 i mejerimjölk för perioden 1955-1990. SSI-rapport 92-20. Stateris strålskyddsinstitut. Stockholm (in Swedish).

Thaning, L. & Baklanov, A. (1997) Simulation of atmospheric transport and deposition on the local/meso- and regional scales after hypothetical accidents at Kola Nuclear Power Plant. *Scien. Tot. Envir.*, **202**, 199-210.

Travnikova, I.G., V.N. Shutov, G.Ya. Bruk, M.I. Balonov et al. (2002) Assessment of current exposure levels in different population groups of the Kola Peninsula, *Journal of Environmental Radioactivity* **60**, 235-248.

Tschiersch, J., F. Trautner and G. Frank. (1995) Deposition of atmospheric aerosol by rain and fog. In: *EC 'Radiation Protection' Report* # EUR 16604 EN, pp. 3-11.

Webler, T., D. Levine, H. Rakel, and O. Renn (1991) A Novel Approach to Reducing Uncertainty: The Group Delphi, *Technological Forecasting and Social Change* **39**(3), 253-263.

Wright, S.M., P. Strand, M. Sickel., B.J. Howard, D.C. Howard, A.I. Cooke (1997) Spatial variation in the vulnerability of Norwegian Arctic counties to radiocaesium deposition. *Science of the Total Environment*, **202**, 173-184.

Wright, S.M., V. Golikov, B. J. Howard, L. Skuterud, A. Baklanov and B. Salbu (2002) Long-term consequences of hypothetical releases from the Kola NPP on the Murmansk oblast in Russia. In: The 5th International conference on Environmental Radioactivity in the Arctic, St-Petersburg, Russia, June 16-20, 2002, NRPA, pp 373-376.

Yamartino, R.J. (1985) Atmospheric pollutant deposition modelling. Chapter 27 in: *Handbook of applied meteorology*. Houghton, D.D., Editor. A Wiley-Interscience Publication. New-York. 754-766 pp.

Zanetti, P. (1990) *Air Pollution Modeling - Theories, Computational Methods and Available Software*. Southampton: Computational Mechanics and New York: Van Nostrand Reinhold.

Zilitinkevich, S. and A. Baklanov (2002) Calculation of the height of stable boundary layers in practical applications. *Boundary-Layer Meteorology*, **105**(3): 389-409.

ABBREVIATIONS

AR-NARP	"Arctic Risk" Project - Nordic Arctic Research Programme
AF	AirFlow
AHHPI	Area of the Highest Probability of the Possible Impact
AMC	Absolute Maximum Cell
ATP	Atmospheric Transport Pathways
BBP	Block of the British NPPs
BGP	Block of the German NPPs
BNP	Barsebaeck Nuclear Power Plant
DERMA	Danish Emergency Response Model for Atmosphere
DMI	Danish Meteorological Institute
ECMWF	European Center for Medium Weather Forecast
FT	Fast Transport
GIS	Geographic Information System
HIRLAM	HIgh Resolution Limited Area Model
INP	Ignalina Nuclear Power Plant
KNP	Kola Nuclear Power Plant
LNP	Leningrad Nuclear Power Plant
LRS	Loviisa Nuclear Power Plant
MPIZ	Maximum Possible Impact Zone
MRD	Maximum Reaching Distance
NCAR	National Center for Atmospheric Research
NCEP	National Center for Environmental Prediction
NPP	Nuclear Power Plant
NRS	Nuclear Risk Site
NZS	Novaya Zemlya Test Site
ONP	Oskarshamn Nuclear Power Plant
PF	Precipitation Factor
RNP	Ringhals Nuclear Power Plant
TRS	Olkiluoto (TVO) Nuclear Power Plant
TTT	Typical Transport Time
UDHR	Unit Discrete Hypothetical Release

DANISH METEOROLOGICAL INSTITUTE

Scientific Reports

Scientific reports from the Danish Meteorological Institute cover a variety of geophysical fields, i.e. meteorology (including climatology), oceanography, subjects on air and sea pollution, geomagnetism, solar-terrestrial physics, and physics of the middle and upper atmosphere.

Reports in the series within the last five years:

No. 97-1
E. Friis Christensen og C. Skøtt: Contributions from the International Science Team. The Ørsted Mission - a pre-launch compendium

No. 97-2
Alix Rasmussen, Sissi Kiilsholm, Jens Havskov Sørensen, Ib Steen Mikkelsen: Analysis of tropospheric ozone measurements in Greenland: Contract No. EV5V-CT93-0318 (DG 12 DTEE):
DMI's contribution to CEC Final Report Arctic Trophospheric Ozone Chemistry ARCTOC

No. 97-3
Peter Thejll: A search for effects of external events on terrestrial atmospheric pressure: cosmic rays

No. 97-4
Peter Thejll: A search for effects of external events on terrestrial atmospheric pressure: sector boundary crossings

No. 97-5
Knud Lassen: Twentieth century retreat of sea-ice in the Greenland Sea

No. 98-1
Niels Woetman Nielsen, Bjarne Amstrup, Jess U. Jørgensen: HIRLAM 2.5 parallel tests at DMI: sensitivity to type of schemes for turbulence, moist processes and advection

No. 98-2
Per Høeg, Georg Bergeton Larsen, Hans-Henrik Benzon, Stig Syndergaard, Mette Dahl Mortensen: The GPSOS project Algorithm functional design and analysis of ionosphere, stratosphere and troposphere observations

No. 98-3
Mette Dahl Mortensen, Per Høeg: Satellite atmosphere profiling retrieval in a nonlinear troposphere Previously entitled: Limitations induced by Multipath

No. 98-4
Mette Dahl Mortensen, Per Høeg: Resolution properties in atmospheric profiling with GPS

No. 98-5
R.S. Gill and M. K. Rosengren: Evaluation of the Radarsat imagery for the operational mapping of sea ice around Greenland in 1997

No. 98-6
R.S. Gill, H.H. Valeur, P. Nielsen and K.Q. Hansen: Using ERS SAR images in the operational mapping of sea ice in the Greenland waters: final report for ESA-ESRIN's: pilot projekt no. PP2.PP2.DK2 and 2nd announcement of opportunity for the exploitation of ERS data projekt No. AO2..DK 102

No. 98-7
Per Høeg et al.: GPS Atmosphere profiling methods and error assessments

No. 98-8
H. Svensmark, N. Woetmann Nielsen and A.M. Sempreviva: Large scale soft and hard turbulent states of the atmosphere

No. 98-9
Philippe Lopez, Eigil Kaas and Annette Guldberg: The full particle-in-cell advection scheme in spherical geometry

No. 98-10
H. Svensmark: Influence of cosmic rays on earth's climate

No. 98-11
Peter Thejll and Henrik Svensmark: Notes on the method of normalized multivariate regression

No. 98-12
K. Lassen: Extent of sea ice in the Greenland Sea 1877-1997: an extension of DMI Scientific Report 97-5

No. 98-13
Niels Larsen, Alberto Adriani and Guido DiDonfrancesco: Microphysical analysis of polar stratospheric clouds observed by lidar at McMurdo, Antarctica

No.98-14
Mette Dahl Mortensen: The back-propagation method for inversion of radio occultation data

No. 98-15
Xiang-Yu Huang: Variational analysis using spatial filters

No. 99-1
Henrik Feddersen: Project on prediction of climate variations on seasonel to interannual timescales (PROVOST) EU contract ENVA4-CT95-0109: DMI contribution to the final report:Statistical analysis and post-processing of uncoupled PROVOST simulations

No. 99-2
Wilhelm May: A time-slice experiment with the ECHAM4 A-GCM at high resolution: the experimental design and the assessment of climate change as compared to a greenhouse gas experiment with ECHAM4/OPYC at low resolution

No. 99-3
Niels Larsen et al.: European stratospheric monitoring stations in the Artic II: CEC Environment and Climate Programme Contract ENV4-CT95-0136. DMI Contributions to the project

No. 99-4
Alexander Baklanov: Parameterisation of the deposition processes and radioactive decay: a review and some preliminary results with the DERMA model

No. 99-5
Mette Dahl Mortensen: Non-linear high resolution inversion of radio occultation data

No. 99-6
Stig Syndergaard: Retrieval analysis and methodologies in atmospheric limb sounding using the GNSS radio occultation technique

No. 99-7
Jun She, Jacob Woge Nielsen: Operational wave forecasts over the Baltic and North Sea

No. 99-8
Henrik Feddersen: Monthly temperature forecasts for Denmark - statistical or dynamical?

No. 99-9
P. Thejll, K. Lassen: Solar forcing of the Northern hemisphere air temperature: new data

No. 99-10
Torben Stockflet Jørgensen, Aksel Walløe Hansen: Comment on "Variation of cosmic ray flux and global coverage - a missing link in solar-climate relationships" by Henrik Svensmark and Eigil Friis-Christensen

No. 99-11
Mette Dahl Meincke: Inversion methods for atmospheric profiling with GPS occultations

No. 99-12
Hans-Henrik Benzon; Laust Olsen; Per Høeg: Simulations of current density measurements with a Faraday Current Meter and a magnetometer

No. 00-01
Per Høeg; G. Leppelmeier: ACE - Atmosphere Climate Experiment

No. 00-02
Per Høeg: FACE-IT: Field-Aligned Current Experiment in the Ionosphere and Thermosphere

No. 00-03
Allan Gross: Surface ozone and tropospheric chemistry with applications to regional air quality modeling. PhD thesis

No. 00-04
Henrik Vedel: Conversion of WGS84 geometric heights to NWP model HIRLAM geopotential heights

No. 00-05
Jérôme Chenevez: Advection experiments with DMI-Hirlam-Tracer

No. 00-06
Niels Larsen: Polar stratospheric clouds microphysical and optical models

No. 00-07
Alix Rasmussen: "Uncertainty of meteorological parameters from DMI-HIRLAM"

No. 00-08
A.L. Morozova: Solar activity and Earth's weather. Effect of the forced atmospheric transparency changes on the troposphere temperature profile studied with atmospheric models

No. 00-09
Niels Larsen, Bjørn M. Knudsen, Michael Gauss, Giovanni Pitari: Effects from high-speed civil traffic aircraft emissions on polar stratospheric clouds

No. 00-10
Søren Andersen: Evaluation of SSM/I sea ice algorithms for use in the SAF on ocean and sea ice, July 2000

No. 00-11
Claus Petersen, Niels Woetmann Nielsen: Diagnosis of visibility in DMI-HIRLAM

No. 00-12
Erik Buch: A monograph on the physical oceanography of the Greenland waters

No. 00-13
M. Steffensen: Stability indices as indicators of lightning and thunder

No. 00-14
Bjarne Amstrup, Kristian S. Mogensen, Xiang-Yu Huang: Use of GPS observations in an optimum interpolation based data assimilation system

No. 00-15
Mads Hvid Nielsen: Dynamisk beskrivelse og hydrografisk klassifikation af den jyske kyststrøm

No. 00-16
Kristian S. Mogensen, Jess U. Jørgensen, Bjarne Amstrup, Xiaohua Yang and Xiang-Yu Huang: Towards an operational implementation of HIRLAM 3D-VAR at DMI

No. 00-17
Sattler, Kai; Huang, Xiang-Yu: Structure function characteristics for 2 meter temperature and relative humidity in different horizontal resolutions

No. 00-18
Niels Larsen, Ib Steen Mikkelsen, Bjørn M. Knudsen m.fl.: In-situ analysis of aerosols and gases in the polar stratosphere. A contribution to THESEO. Environment and climate research programme. Contract no. ENV4-CT97-0523. Final report

No. 00-19
Amstrup, Bjarne: EUCOS observing system experiments with the DMI HIRLAM optimum interpolation analysis and forecasting system

No. 01-01
V.O. Papitashvili, L.I. Gromova, V.A. Popov and O. Rasmussen: Northern polar cap magnetic activity index PCN: Effective area, universal time, seasonal, and solar cycle variations

No. 01-02
M.E. Gorbunov: Radioholographic methods for processing radio occultation data in multipath regions

No. 01-03
Niels Woetmann Nielsen; Claus Petersen: Calculation of wind gusts in DMI-HIRLAM

No. 01-04
Vladimir Penenko; Alexander Baklanov: Methods of sensitivity theory and inverse modeling for estimation of source parameter and risk/vulnerability areas

No. 01-05
Sergej Zilitinkevich; Alexander Baklanov; Jutta Rost; Ann-Sofi Smedman, Vasiliy Lykosov and Pierluigi Calanca: Diagnostic and prognostic equations for the depth of the stably stratified Ekman boundary layer

No. 01-06
Bjarne Amstrup: Impact of ATOVS AMSU-A radiance data in the DMI-HIRLAM 3D-Var analysis and forecasting system

No. 01-07
Sergej Zilitinkevich; Alexander Baklanov: Calculation of the height of stable boundary layers in operational models

No. 01-08
Vibeke Huess: Sea level variations in the North Sea – from tide gauges, altimetry and modelling

No. 01-09
Alexander Baklanov and Alexander Mahura: Atmospheric transport pathways, vulnerability and possible accidental consequences from nuclear risk sites: methodology for probabilistic atmospheric studies

No. 02-01
Bent Hansen Sass and Claus Petersen: Short range atmospheric forecasts using a nudging procedure to combine analyses of cloud and precipitation with a numerical forecast model

No. 02-02
Erik Buch: Present oceanographic conditions in Greenland waters

No. 02-03
Bjørn M. Knudsen, Signe B. Andersen and Allan Gross: Contribution of the Danish Meteorological Institute to the final report of SAMMOA. CEC contract EVK2-1999-00315: Spring-to.-autumn measurements and modelling of ozone and active species

No. 02-04
Nicolai Kliem: Numerical ocean and sea ice modelling: the area around Cape Farewell (Ph.D. thesis)

No. 02-05
Niels Woetmann Nielsen: The structure and dynamics of the atmospheric boundary layer

No. 02-06
Arne Skov Jensen, Hans-Henrik Benzon and Martin S. Lohmann: A new high resolution method for processing radio occultation data

No. 02-07
Per Høeg and Gottfried Kirchengast: ACE+: Atmosphere and Climate Explorer

No. 02-08
Rashpal Gill: SAR surface cover classification using distribution matching

No. 02-09
Kai Sattler, Jun She, Bent Hansen Sass, Leif Laursen, Lars Landberg, Morten Nielsen og Henning S. Christensen: Enhanced description of the wind climate in Denmark for determination of wind resources: final report for 1363/00-0020: Supported by the Danish Energy Authority

No. 02-10
Michael E. Gorbunov and Kent B. Lauritsen: Canonical transform methods for radio occultation data

No. 02-11
Kent B. Lauritsen and Martin S. Lohmann: Unfolding of radio occultation multipath behavior using phase models

No. 02-12
Rashpal Gill: SAR image classification using fuzzy screening method

No. 02-13
Kai Sattler: Precipitation hindcasts of historical flood events

No. 02-14
Tina Christensen: Energetic electron precipitation studied by atmospheric x-rays

No. 02-15
Alexander Mahura and Alexander Baklanov: “Probablistic analysis of atmospheric transport patterns from nuclear risk sites in Euro-Arctic Region”

No. 02-16
A. Baklanov, A. Mahura, J.H. Sørensen, O. Rigina, R. Bergman: Methodology for risk analysis based on atmospheric dispersion modelling from nuclear risk sites